PHYSICAL REVIEW B **75**, 195342 (2007)

Elastic spin-relaxation processes in semiconductor quantum dots

Y. G. Semenov and K. W. Kim
Department of Electrical and Computer Engineering, North Carolina State University, Raleigh, North Carolina 27695-7911, USA

(Received 13 December 2006; revised manuscript received 13 April 2007; published 30 May 2007)

Electron-spin decoherence caused by elastic spin-phonon processes is investigated comprehensively in a zero-dimensional environment. Specifically, a theoretical treatment is developed for the processes associated with the fluctuations in the phonon potential as well as in the electron precession frequency through the spin-orbit and hyperfine interactions in the semiconductor quantum dots. The analysis identifies the conditions (magnetic field, temperature, etc.) in which the elastic spin-phonon processes can dominate over the inelastic counterparts with the electron spin-flip transitions. Particularly, the calculation results illustrate the potential significance of an elastic decoherence process originating from the intervalley transitions in semiconductor quantum dots with multiple equivalent energy minima (e.g., the X valleys in SiGe). The role of lattice anharmonicity and phonon decay in spin relaxation, including the zero-point quantum effect, is examined along with that of the local effective-field fluctuations caused by the stochastic electronic transitions between the orbital states. Numerical estimations are provided for typical GaAs- and Si-based quantum dots.

DOI: 10.1103/PhysRevB.75.195342 PACS number(s): 78.66.−w, 72.20.Ht, 85.60.Dw, 42.65.Pc

I. INTRODUCTION

Electron-spin relaxation in semiconductor quantum dots (QDs) has received much attention as they are a natural candidate for the qubit in quantum computing (QC) (see Refs. 1 and 2 for a brief review). Particularly, a significant effort has been devoted to investigate the spin transition probabilities associated with the spin-flip interactions, for example, the so-called longitudinal spin relaxation (T_1) (i.e., energy relaxation) induced via the inelastic process of phonon absorption and/or emission by an electron spin localized in a QD. Although generally an important source of decoherence, the spin-flip events can sometimes be efficiently suppressed by an appropriate choice of external conditions including the magnetic-field strength or direction. In this case, alternative mechanisms (such as the elastic spin-phonon scattering that does not assume energy exchange between the electron Zeeman energy and thermal bath) can be primarily responsible for decoherence. So far, however, the elastic processes have received relatively little attention. This disparity may be due, in part, to the mathematical simplicity in the treatment of the former case (e.g., calculations based on Fermi's golden rule), while the elastic processes of spin decoherence need more sophisticated approaches. At the same time, recent proliferation of the literature on electron-spin relaxation has exacerbated the confusion on this complicated subject matter. Frequently, an individual study addresses only a specific aspect of spin decoherence or dephasing without elucidating its place in the general theory or the interrelationships with other relevant works. Consequently, one faces difficulties each time in determining which existing mechanisms, processes, or theories are relevant for spin relaxation under the given external conditions and specific QD properties.

The purpose of the present study is to systematically identify and analyze the crucial transversal (T_2) spin-relaxation processes in the context of qubit dephasing in the electron-spin-based QC. Specifically, the role of spin-phonon interaction on the elastic decoherence processes is examined theoretically from the perspective of the fluctuations in the effective magnetic field. The calculation identifies the conditions in which the elastic spin-lattice processes can dominate over the inelastic counterparts. The analysis is applicable to the electron spin in both group IV and III-V QDs. Note that the related issues from the spintronics point of view were surveyed in Refs. 3 and 4.

The rest of this paper is organized as follows. Section II provides a systematic classification of most, if not all, of the processes identified so far that lead to a type of electron-spin relaxation (i.e., dephasing, decoherence, or energy relaxation). Then, the discussion focuses on those caused by the spin-phonon interaction and describes different manifestations of the spin-phonon interaction in a manner consistent to both elastic and inelastic processes. Subsequently, the elastic decoherence processes that warrant further analysis are recognized and their potential significance outlined in the context of QC. Section III summarizes the theoretical framework, while the detailed mathematical treatment of electron-spin relaxation in terms of quantum kinetic equation is discussed in the Appendix.

Each of the following three sections describes a particular elastic process that can be dominant under a certain condition. In Sec. IV, we analyze the effects of spin precession fluctuations due to the irregular phonon phase disturbances originating from phonon relaxation via the lattice anharmonicity or imperfections. Such a situation applies not only to real (thermally activated) phonons but also to the zero-point vibrations (or quantum effects) that the classical picture cannot address. Section V considers spin phase diffusion due to the modulations in the longitudinal g tensor and hyperfine interaction through the phonon-assisted transitions between the lowest electronic states (without spin flip). Section VI concerns electron spin in a semiconductor QD with multiple equivalent minima (e.g., $\mathrm{Si}_{1-x}\mathrm{Ge}_x$). As the degeneracy is lifted due to structural inversion asymmetry, phonon-mediated transitions between the "valley-split" states can be allowed when the local crystal imperfections are present. This process can be very significant since the energy separation of the valley-split states is generally comparable to the thermal energy in the QC operation. Then, the discussion on

TABLE I. Main contributions to electron spin-dephasing (with T_2^*) in a QD spin-based QC system. The "random local fields" category denotes the processes that lead to phase diffusion of the multiqubit system without causing decoherence in the individual qubits (i.e., spin). The decoherence or transversal relaxation (T_2) has contributions from both elastic and inelastic processes for a single spin. The latter involves spin-flip transitions leading to the energy (or longitudinal) relaxation of the spin states (i.e., T_1). The # sign denotes the spin-relaxation processes induced by the spin-phonon interactions. HFI symbolizes the hyperfine interaction.

Dephasing (T_2^*)		
Decoherence (T_2)		
Inelastic process (T_1)	Elastic process	Random local fields
Direct spin flip#	Anharmonic vibration#	g-tensor dispersion
Orbach#	Local-field steps#	Dispersion of HFI
Two phonon#	Spectral diffusion	Impurity fields
Nuclear spins	Geometric phase#	Interqubit interaction

the comparative importance of different processes in the parameter space is provided in Sec. VII with a Si QD as an example, followed by a brief conclusion in Sec. VIII.

II. SPIN-RELAXATION PROCESSES AND MECHANISMS

For a systematic analysis, Table I shows a simple classification of the relevant spin-relaxation processes identified so far. The term "dephasing" (with the characteristic time T_2^*) concerns the phase relaxation of a QC system consisting of multiple qubits, while "decoherence" (T_2) is for a single qubit (i.e., single-electron spin in a QD). Hence, decoherence contributes to dephasing ($T_2 \geqslant T_2^*$). The "random local fields" category denotes the processes that lead to phase diffusion of the multiqubit system without causing decoherence in the individual qubits. The decoherence or transversal relaxation has contributions from both the elastic and inelastic processes. The latter involves spin-flip transitions leading to the energy (or longitudinal) relaxation of the spin states (i.e., T_1). Of the spin decoherence processes, those marked by the # sign in the table are induced by the spin-phonon interaction. The listed T_2 processes correspond to the uncontrollable interactions with the environment that are assumed to be in a thermodynamic equilibrium at temperature T. Inaccuracies in the parameters of the control pulses during QC operations as well as uncontrollable perturbations introduced with these pulses (see, for example, Ref. 5) are beyond the current description. Table II summarizes various manifestations of the spin-phonon mechanism in a manner consistent to both elastic and inelastic processes. A brief description on each category is given below.

A. Dephasing in random fields

The fastest relaxation in a quantum computer consisting of a large number of qubits [$N \sim 1000$ (see Ref. 2)] is the dephasing process associated with transversal magnetization loss with the characteristic time T_2^*. Clearly, the electrons experience a dispersion of spin precession in the presence of a random effective magnetic field. Even when the magnetic field can be considered a constant spatially and temporally for a given qubit within the time scale of QC operation, its random variation across the ensemble of qubits can induce dephasing of the system. Although some of its effect may be potentially mitigated by QC algorithms,[2,6] the absence of this additional complexity provides an obvious advantage.

One reason for the dispersion in the precession frequency is the g-tensor variation over the N qubits. Consequently, even in a very pure crystal, the unavoidable fluctuation in the QD sizes results in the dispersion Δg, which subsequently induces dephasing with the rate of $T_{gt}^{*-1} = \Delta g \mu_B B$ (where μ_B is the Bohr magneton and B the external magnetic field). A related case of two-dimensional hole localization in a fluctuating potential was studied in Refs. 7 and 8. In addition, the randomness of spin-orbital coupling in a quantum well due to the fluctuation of dopant concentration was considered in Ref. 9.

TABLE II. Various mechanisms of the spin-phonon interaction in a manner consistent to both elastic and inelastic processes listed in Table I (marked by #). SOI and HFI denote the spin-orbit and hyperfine interactions, respectively.

	Spin-phonon interaction mechanisms		
	Spin-orbit interaction	Hyperfine interaction	Spin-spin interaction
Direct	SOI modulation	HFI modulation	Waller/Exchange modulation
Admixture	Kronig-Van Vleck	Spin state mixing	Spin state mixing
Indirect	g-tensor fluctuation	Hyperfine field fluctuation	Spin-spin fluctuation

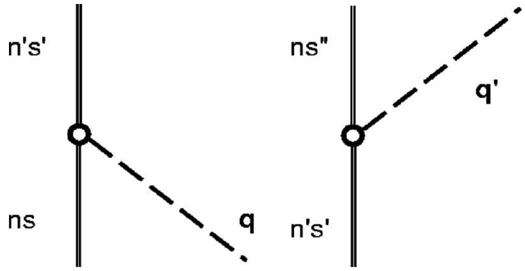

FIG. 1. Diagrams of one-phonon spin-relaxation process. The vertical lines correspond to the localized electrons with orbital n, n' and spin $s = \uparrow, \downarrow$ states; the dashed lines depict a phonon with the $\mathbf{q}$ or $\mathbf{q}'$ mode; and the circle represents a direct electron-phonon interaction. When the electronic transition due to the interaction with a phonon does not change the orbital states (i.e., $n = n'$), the diagrams describe the direct process of spin relaxation with the absorption (left panel) or the emission (right panel) of the phonon resonant with the Zeeman splitting. If n and n' correspond to the ground and excited states, respectively, the net effect of two depicted processes in tandem represents the Orbach process of spin relaxation. In this case (Orbach), the spin flip occurs only in one of the stages (either absorption or emission), while the other is spin independent.

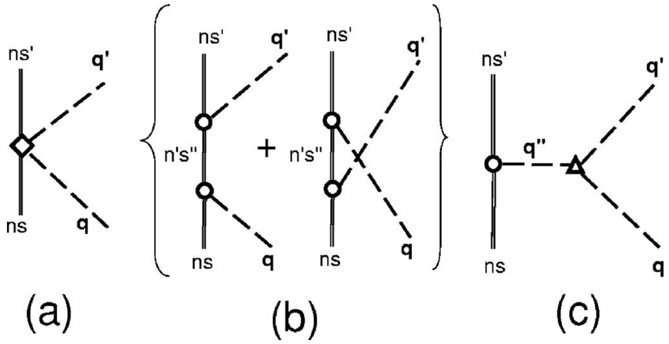

FIG. 2. Diagrams describing three types of spin flip $s \rightarrow s'$ Raman processes under the inelastic two-phonon scattering. (a) The spin–two-phonon interaction in the first order results in the direct Raman spin-relaxation process. (b) The process of second order on the one-phonon interactions assumes the electronic virtue transitions via intermediate states $n's''$; the interference of the processes, which corresponds to the braced diagrams, sometimes leads to the so-called Van Vleck cancellation and the distinctive dependence $\sim T^9$ for the relaxation rate. (c) The anharmonic spin-relaxation Raman process implies an inelastic phonon scattering due to the third-order anharmonicity with the creation of a virtual phonon q'', which in turn induces a spin flip via the spin–one-phonon interaction. Processes (a) and (c) are characterized by typical temperature dependence $\sim T^7$ for the Raman spin-relaxation rate. As explained, the square represents the direct spin–two-phonon interaction, while the triangle stands for the inelastic phonon scattering due to the third-order anharmonicity; other notations are the same as in Fig. 1.

Similarly, electron interaction with nuclear spins can induce the spin phase diffusion due to the random distribution of the nuclear-spin states and their spatial locations.[10–12] In principle, replacement of the magnetic isotopes by nonmagnetic counterparts $(I=0)$ can remove or suppress this source of relaxation.[13] However, it may not be a practical option as a significant level of purification is required to be effective; the dephasing rate depends only weakly on the nuclear-spin concentration n_I (i.e., $\propto \sqrt{n_I}$). As indicated in Table I, the random fields of magnetic impurities also contribute to the dephasing process. The last one listed in this category, the magnetodipole interaction between the qubits, plays a specific role since it can be incorporated (thus, eliminated) to the QC algorithm under certain conditions.[2,14,15]

B. Inelastic processes

Among the inelastic processes in Table I, the direct spin-flip via one-phonon emission and/or absorption (see Fig. 1) is the most studied due to its simplicity in concept as well as its importance at low temperatures.[16–21] The rate of this process is proportional to the phonon density of states $g(\omega_q)$ $(\sim \omega_q^2)$ at the resonant phonon energy $\hbar\omega_q = g\mu_B B$ $(\equiv \hbar\omega)$ as well as to the square of the spin-phonon matrix element $(\sim \omega_q B^2)$. As a result, a strong magnetic-field dependence $(\sim B^5)$ is expected for the direct spin flip. Thus, at low magnetic fields, the effect of this process can be significantly reduced. When $k_B T < \hbar\omega$, the influence of the temperature can be ignored as the phonon emission determines the relaxation rate.

The Orbach process[22,23] considers the spin-flip events through successive transitions between the ground and excited orbital states separated by an energy δ_0. For example, an electron first makes a spin-flip transition to the excited state with opposite spin by absorbing a phonon with energy $\delta_0 \mp \hbar\omega$, followed by a return to the ground state through emission of a phonon with energy δ_0. An alternative channel is to make a transition to the excited state without spin flip (i.e., δ_0) and then return to the ground state with opposite spin (i.e., $\delta_0 \mp \hbar\omega$). Thus, the net effect is the electron spin flip with the energy of $\hbar\omega$ (i.e., the Zeeman splitting) transferred to the thermal bath. Under certain conditions, the corresponding matrix elements can exceed those for the direct spin-flip transitions between the Kramers doublet.[24] It should be stressed that the Orbach process assumes two one-phonon transitions in tandem. Hence, the first transition with the energy threshold of $\delta_0 \mp \hbar\omega$ or δ_0 provides the primary temperature dependence along with a weak influence of the magnetic field.

The two-phonon process concerns the longitudinal spin relaxation via two-phonon absorption or emission or inelastic phonon scattering (Raman process). It can be further divided into three groups: the direct spin two-phonon transitions due to the nonlinearity of the spin-phonon Hamiltonian[25] [Fig. 2(a)], the virtual transitions mediated by one-phonon interactions through the excited states[16,18] [Fig. 2(b)], and the anharmonic Raman process[26,27] [Fig. 2(c)]. In the case of virtual transitions, the integration over phonons includes the poles at the phonon energy $\hbar\omega_q \sim \delta_0$ if $\delta_0 < k_B\Theta$, where Θ is the Debye temperature. The treatment of this singularity (the so-called phonon resonant fluorescence) beyond the conventional perturbation theory[28] involves essentially the finite lifetime τ_R of the excited states that exactly reproduces the relaxation rate of the Orbach process.[22,29] This coincidence and/or similarity is lifted (i.e., the poles can be ignored as compared to the Orbach process) when the finite phonon lifetime τ_q is considered since $\tau_R^{-1} \ll \tau_q^{-1}$. As the processes involving the inelastic two-phonon scattering show a strong dependence on temperature ($T^7 - T^{11}$),[16,18] it has been mostly ignored in the consideration of QC that operates at very low temperatures. However, a recent analysis[18] suggests its potential significance in the low-magnetic-field regime due to the weak dependence on the field strength (B^2).

The process of directly transferring the electron Zeeman energy to the nuclear dipole-dipole reservoir is another possible channel for longitudinal relaxation.[30] This, however, can be effective only in the external magnetic fields comparable to or weaker than the local nuclear fields, which are generally sufficiently small. In addition to those listed in Table I, the simultaneous flip-flop of several spins generally entails energy exchange with the phonon or spin-spin reservoir. Much less attention has been paid to such processes in the literature.[31–33]

C. Elastic processes

The elastic processes can be imagined as a result of uncontrollable fluctuations of Zeeman frequency or its equivalent, i.e., the fluctuations of longitudinal magnetic field that conserve the electron-spin projection on the quantization axis. As summarized in Table I, there are at least four different manifestations of this process. Of these, the first one listed ("anharmonic vibration") represents the case where the irregular phonon phase disturbances originating from the phonon relaxation induce a net effect of electron-spin phase decay via the spin-phonon interaction. If the phonons are treated as ideal quasiparticles without damping, the longitudinal component of the "effective" interaction field takes the form of a harmonic perturbation and does not cause alteration in the electron-spin phase.[34] [One exception may be the small spin phase decoherence ($\sim 10^{-9}$) that can be acquired under the additional assumption of identical phase for all the harmonic phonon modes at the initial instant.[35]] However, a different situation can be realized when the phonon oscillation is interrupted by a series of random-phase disturbances, as schematically illustrated in Fig. 3. The reason of such phonon phase steps can be lattice anharmonicity, phonon scattering at the impurities or lattice defects, etc. These irregular phonon phase perturbations affect the electron-spin precession resulting in its phase relaxation.[34]

The fluctuations in the local effective magnetic field (and, thus, spin decoherence) can also result from the transitions between the electronic (orbital) states with different Zeeman frequencies. As the electron experiences the stochastic transitions between these orbital states without spin flip, electron-spin phase can change due to the finite and random lifetime in the states with different precession frequencies.[36] It should be emphasized that although the transitions are mediated by phonons, the energy exchange between the Zeeman and phonon reservoirs does not take place in contrast to the Orbach process; i.e., this case undoubtedly belongs to the elastic processes.

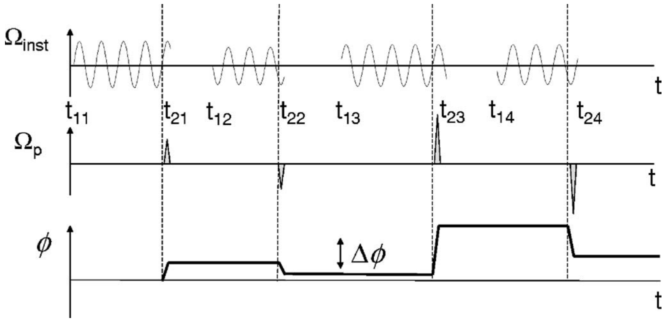

FIG. 3. Schematic illustration of a single-phonon contribution to the random spin phase shift. Ω_{inst} is the instantaneous effective field of spin precession associated with a phonon. $t_{11}, t_{12}, t_{13}, \ldots$, are the random instants of phonon generation, while $t_{21}, t_{22}, t_{23}, \ldots$, are of phonon annihilation. The vertical dotted lines depict the instants of the last full oscillations by the phonon before its disappearance. The residual oscillations (on the right of the dotted line) are not compensated and produce the net effect (Ω_p), which influences the spin as a short pulse with a random amplitude at random times. The phase shift due to the influence of Ω_p is a Markovian process at the time interval $t \gg \tau_c$, where the phonon correlation time τ_c is defined as a mean value of the differences $t_{1i+1} - t_{1i}$ (thus, $\tau_c = \tau_p$, the phonon relaxation time). The phase relaxation time is proportional to the mean value of the squared phase shift caused by a single pulse $\langle \Delta\phi^2 \rangle$ and the rate of phonon relaxation τ_p^{-1}.

Electron spin can accumulate the phase shift through random thermal changes in the nuclear-spin distribution as well. Although a quantum state of individual nuclear spin generally has a relatively long lifetime, a large ensemble of nuclear spins (or spin-flip transitions) produces a rapidly evolving effective-field distribution. Its significance can be gauged in terms of electron resonant frequency diffusion (i.e., the so-called spectral diffusion) in the spin-echo experiments.[13,37–40] A peculiar property of this process is the cubic exponential decay of spin-echo signal $\sim \exp[-t^3/T_M^3]$, where the memory time T_M can be calculated in the model of uncorrelated nuclear-spin flips[39] or by taking into account the flip-flop processes for nuclear-spin pairs.[40] Recent investigations, however, provide corrections to this dependence with a more general result for spin-coherence evolution $\sim \exp[-t^n/T_{2,hf}^n]$.[41–43] In Ref. 41, the straightforward quantum-mechanical attack to the problem was performed in terms of the pair-correlation approximation that yields $n=4$ (i.e., $\sim \exp[-t^4/T_{2,hf}^4]$); in doing so, the indirect nuclear-spin interaction via electron spin was incorporated into the spin dynamics calculation along with the direct dipole-dipole interaction. Moreover, an approach based on the electron-spin correlation function and a model Hamiltonian for hyperfine interaction was proposed[42] and a cluster method developed for the secular part of the interaction Hamiltonian under strong magnetic fields (~ 10 T).[43] The latter method reproduces the result of Ref. 41 in the case of GaAs QD and defines more precisely the spin-echo signal decay of shallow donors in Si with $n=2.3$. Note, however, that the spectral diffusion process is probably irrelevant to QC, where only the initial phase decay of $\varepsilon \sim 10^{-4} - 10^{-6}$ matters for fault tolerant operation. In the corresponding short time frame, the processes with a linear exponential decay $\exp[-t/T_2]$ prevail (unless $T_{2,hf} < \varepsilon^{1-1/n} T_2$), as was experimentally demonstrated in Ref. 13. Decoherence can also be attributed to isolated (i.e., noninteracting) nuclear spins.[44] This is because each nuclear spin precesses around the electron hyperfine field, which is inhomogeneous over the QD volume. Such uncorrelated nuclear-spin precession, in turn, leads to the change in the strength of nuclear hyperfine interaction field affecting the electron spin and its phase. The efficiency of this process, however, is much weaker than that of spectral diffusion when the internuclear interaction is taken into account.

The elastic processes in Table I include the one mediated by fluctuations of the Berry geometric phase.[45–47] The efficiency of this process compared to the others is not clearly understood yet. In addition, an elastic phonon scattering on a group of spins can cause them to be out of phase.[32,33] However, this process is less relevant for single qubit decoherence.

D. Mechanisms of spin-phonon interaction

Table II summarizes the microscopic mechanisms of spin-phonon interaction that give rise to the elastic and inelastic spin-relaxation processes (marked by # in Table I). Despite the great multiplicity of the mechanisms considered in the literature, they can be classified into three groups following the global characteristics, i.e., the mechanisms resulting from the (i) spin-orbit, (ii) hyperfine, and (iii) spin-spin interactions. In turn, these interactions manifest themselves in a number of different ways, all of which can contribute to spin phase and longitudinal relaxations.

Taking into account that interactions (i)–(iii) mentioned above possess, generally speaking, nonzero matrix elements between the states appurtenant to the Zeeman doublet, their modulation by phonon vibrations can be expressed as a Hamiltonian realizing the spin-phonon interaction (listed as "Direct" in Table II). Mathematically, if a phonon mediates an electronic potential $V_{ph}(\mathbf{r})$, the spin-orbit interaction is changed by the term $H_{so\text{-}ph}=\frac{\hbar}{2m^2c^2}[\nabla V_{ph}\times\mathbf{p}]\mathbf{s}$ ("SOI modulation" mechanism). At the same time, the shift $\Delta\mathbf{R}_j$ of an atomic position from the site $\mathbf{R}_j$ due to the lattice vibration (i.e., phonons) also changes the Hamiltonian for the hyperfine interaction $H_{hf}(\mathbf{R}_j)=\Sigma_j\mathbf{s}\hat{\mathbf{a}}_{hf}(\mathbf{r}-\mathbf{R}_j)\mathbf{I}$ by $H_{hf\text{-}ph}=H_{hf}(\mathbf{R}_j+\Delta\mathbf{R}_j)-H_{hf}(\mathbf{R}_j)$ ("HFI modulation" mechanism); here, $\hat{\mathbf{a}}_{hf}(\mathbf{r}-\mathbf{R}_j)$ is the hyperfine interaction tensor. The case of spin-orbit interaction adapted to the QDs was considered in Ref. 16. Direct phonon fluctuations of hyperfine interaction were studied for a donor in silicon,[48] F centers in alkali halides,[25] and adapted to QDs.[49]

In a similar manner, one can introduce the spin-phonon interaction mediated by the spin-spin interactions $H_{ss\text{-}ph}$. In this case, one can further separate the dipole-dipole and exchange interactions. Obviously, these mechanisms depend on the interspin distances. Phonon modulation of dipole-dipole interaction ("Waller" mechanism) was considered in Ref. 50, whereas the role of exchange interaction including the Dzyaloshinskii-Moriya terms[51,52] was analyzed in Ref. 31. Particularly, the Dzyaloshinskii-Moriya interaction that mixes the spin states results in effective spin relaxation under the phonon-induced modulation of the isotropic exchange Hamiltonian[53] and can be important in crystals with no inversion symmetry.[54]

The direct mechanisms considered above are not the only manifestation of the spin-phonon interactions. In the strict sense, the Kramers doublets actually represent nonmultiplicative functions of spin and space variables due to the spin-orbit or hyperfine interactions (i.e., mixing of orbital and spin states; "Admixture" in Table II). This makes a spin-independent phonon potential capable of evoking the transitions between the Kramers doublet. Such a mechanism becomes apparent in the case of hole spin relaxation in a QD, where the spin-orbit interaction imposes a linear combination of different spin and orbital states for the basis of valence band.[55,56] Mathematically, the mechanism constitutes only the nonzero matrix elements $\langle g\uparrow|V_{ph}(\mathbf{r})|g\downarrow\rangle$ that can be symbolically transformed to the form

$$\sum_{\{e\}}\left[\frac{\langle g\uparrow|V_{ph}(\mathbf{r})|e\uparrow\rangle\langle e\uparrow|H_{mix}|g\downarrow\rangle}{E_g-E_e}+\frac{\langle g\uparrow|H_{mix}|e\downarrow\rangle\langle e\downarrow|V_{ph}(\mathbf{r})|g\downarrow\rangle}{E_g-E_e}\right] \tag{1}$$

if a perturbation theory is applicable for the system, with the electron energies E_g and E_e in the ground ($|g\rangle$) and excited ($|e\rangle$) states; ↑ and ↓ denote different spin states. Equation (1) assumes that the diagonal part of the Hamiltonian H_{mix} enters into E_g and E_e, while the off-diagonal element mixes the ground and excited states with opposite spins.

In the second-order perturbation theory, Eq. (1) represents the spin-phonon interaction as the process of virtual transition to the spin-flip excited state due to H_{mix} followed by a transition to the ground state without spin flip via the spin-independent electron-phonon interaction, or vice versa. In the case of an electron in a QD, this mechanism can possess an advantage over the direct spin-phonon interaction due to the relatively strong spin coupling between the non-Kramers (i.e., orbital) states. It is particularly so when a Zeeman level of the ground state (e.g., $|g\uparrow\rangle$) is nearly degenerate with that of an exited state (e.g., $|e\downarrow\rangle$). Although highly undesirable for QC, this situation can occur in a relatively strong magnetic field[55] or if coupled resonantly to adjacent QDs via tunneling (the "hot spot" effect).[57,58] As a distinctive feature of the admixture spin-phonon interactions is their proportionality to the matrix elements of electron-phonon interaction between the ground and excited states, they can be further classified based on the types of electron-phonon interactions as well as on the potentials that cause an effective mixture of the ground and excited states.

The mechanism caused by simultaneous manifestation of spin-orbit and spin-independent electron-phonon interactions was initially developed by Kronig[59] and Van Vleck[60] for magnetic ions. Adaptation of this "Kronig–Van Vleck" mechanism to the conduction electrons in a QD can be conveniently achieved by extracting the spin-orbit coupling in the form of the Rashba and Dresselhause terms (which efficiently mix the QD ground and excited states).[61,62] Then, the phonon potential of various origins such as the deformation potential, piezoelectric potential,[16,19–21] or the ripple effect at the QD interface[63] gives rise to the effective spin-phonon coupling in the second order. The spin-orbit coupling in the valence band is generally much stronger; hence, *holes* are less attractive as a qubit.[55,56]

When H_{mix} is due to the hyperfine interaction, the spin flip can be considered in a manner similar to that with the spin-orbit interaction as discussed in Refs. 49 and 64; an isomorphous case of a diluted magnetic semiconductor QD was also investigated.[65] It seems that this admixture spin-phonon interaction can be more effective than the direct counterpart (i.e., phonon modulation of the hyperfine interaction). As to the spin-spin interactions (both dipole-dipole and exchange), they can also induce the mixing of spin and orbital states similarly.[53]

In addition to the direct and admixture mechanisms discussed above, one can consider an "indirect" manifestation of spin-dependent interactions. This group of mechanisms accounts for the random fluctuations in the effective field through the phonon-mediated stochastic transitions between different orbital states. As the characteristics of g tensor, hyperfine field, or spin-spin interactions vary with the orbital states, electrons experience uncontrollable changes in these parameters while undergoing spin-independent phonon scattering between them. Such fluctuations cause the transversal relaxation of electron spin[36] along with a potential contribution to the longitudinal relaxation. However, the latter (i.e., spinflip) is expected to be small due to the negligibly small influence on the spectral density at typical Zeeman frequencies.

Finally, there is a higher-order phonon-mediated mechanism that can affect the spin relaxation. Although the phonon potential $V_{ph}(\mathbf{r})$ cannot influence spin precession directly, its incorporation with the electron potential $V_0(\mathbf{r})$, which contributes to the g tensor in a different manner,[66,67] results in a specific spin-phonon interaction $H_{g\text{-}ph} = \Sigma(\delta g_{ij}/\delta V_0)V_{ph}(\mathbf{r})\mu_B B_i s_j$, where s_j are the components of electron-spin operator. This mechanism was analyzed in a QD with respect to the Orbach spin-flip processes[16] as well as in a bulk semiconductor.[68]

In summarizing the possible mechanisms of spin-phonon interaction, it must be pointed out that all of them make *correlated* contributions to the processes marked # in Table I. For example, the direct spin-flip process is caused by the phonon-induced fluctuation of the effective magnetic field (with the resonant frequency $\hbar\omega$) that results from additive contributions of the spin-phonon mechanisms listed in Table II (i.e., the spin-orbit, hyperfine, and spin-spin interactions). Consequently, the corresponding matrix elements of individual mechanisms must be summed before the probability of any process is calculated. Although the importance of interference for certain mechanisms was already discussed in Refs. 19 and 69, it requires further theoretical scrutiny. However, the anticipated difficulty may be circumvented for reasonably weak magnetic fields if the spin-phonon Hamiltonian $H_{s\text{-}ph}$ is considered in terms of a phenomenological tensor $\mathbf{A}$ following the analysis of Ref. 70. This parameter $\mathbf{A}$ is designed to represent the net and/or total contribution of the spin-orbit mechanisms and can be found experimentally from the dependence of electron paramagnetic resonance signal on the applied stress.

As for the contributions of different processes (Table I) to spin relaxation, they do not interfere and, thus, can be considered independently. As mentioned earlier, the present paper investigates dominant elastic spin-relaxation processes via the spin-phonon mechanisms, particularly those originated from the spin-orbit and hyperfine interactions.

III. THEORETICAL FRAMEWORK FOR ELECTRON-SPIN EVOLUTION

It is convenient to represent the Hamiltonian of one-electron system in terms of the effective spin operator $\mathbf{s}$ for the Kramers doublet $\{g\}=\{|g\rangle,|\tilde{g}\rangle\}$ of the ground electronic state. The linear magnetic splitting of Kramers doublet $\{g\}$ is described by an effective Hamiltonian in the common form $H_S = g_{\mu\nu}\mu_B B_\mu s_\nu$, where the g tensor $g_{\mu\nu}$ is introduced. Similarly, the electron-spin interaction H_{SL} with the thermal bath (of Hamiltonian H_L) is expressible as a linear form of the spin operators, $H_{SL} = \mathbf{\Omega}^{(g)}\mathbf{s}$ if only the states $\{g\}$ are involved in the relaxation. Actually, H_{SL} also describes the transitions between different Kramers doublets. If these transitions from the ground $\{g\}$ to excited $\{e\}$ states are virtual (as is the case at sufficiently low temperatures $kT \ll \delta_0$, where δ_0 is the energy separation between the $\{g\}$ and $\{e\}$ states), reduction of the Hamiltonian H_{SL} to the basis $\{g\}$ of spin operators $\mathbf{s}$ poses no specific problem. For example, the off-diagonal elements of H_{SL} between $\{g\}$ and $\{e\}$ states can be eliminated through the procedure of canonical transformation. Hence, the evolution of the spin system at low temperatures is fully described by an effective 2×2 Hamiltonian in the basis of eigenvectors of s_z,

$$H = H_S + H_L + H_{SL}. \tag{2}$$

This Hamiltonian can also be applicable to the cases other than at low temperatures. Note that the problems involving a group of Kramers doublets (e.g., $\{n\}=\{g\},\{e\}$) sometimes allow description by an effective Hamiltonian H_S^{eff} with $\langle\{n\}|H_S^{\text{eff}}|\{n'\}\rangle = \delta_{n,n'}(E_n + g_{\mu\nu}^{(n)}\mu_B B_\mu s_\nu)$ and $\langle\{n\}|H_{SL}|\{n'\}\rangle = (\hat{\mathbf{\Omega}})_{n,n'}\mathbf{s}$; here, the matrix of orbital energy $\delta_{n,n'}E_n$ can alternatively be considered a part of H_L as well. Hence, this case leaves room for the Hamiltonian in the form of Eq. (2) even at elevated temperatures.

With the mechanisms responsible for the spin-phonon interaction H_{SL} ascertained in Table II, the evolution of electron spin can be described according to the rubrics under "Decoherence (T_2)" in Table I. In contrast to the calculation of H_{SL} that requires individualized treatments for each mechanism, most processes, elastic and inelastic, marked by # in Table I (with the exception of "geometric phase" process) can be approached by a general formalism based on kinetic equations. The most general analysis of electron-spin evolution (including the decoherence) can be realized by the spin-density matrix, for which a formally exact equation can be derived based on the projection operator technique. Although this equation is too complicated to solve, it allows further expansion in terms of the interaction Hamiltonian H_{SL} whose bilinear terms correspond to the first Born approximation. Reduction to the Markovian kinetic equation (i.e., no memory effect) can also be achieved in the first Born approximation if one assumes that the correlation functions of the operators of the thermal bath H_L decay with a characteristic time τ_c shorter than the spin-relaxation times T_1 and

T_2. As our consideration is restricted to the case of $s=1/2$, further simplification consists of deriving a closed set of equations for spin vector **S** with three components $\mathbf{S}=\{X,Y,Z\}$: $\langle s_x \rangle \equiv X$, $\langle s_y \rangle \equiv Y$, and $\langle s_z \rangle \equiv Z$, which unambiguously determine the spin-density matrix. If the correlation in the spin relaxation of different components **S** can be ignored, these equations resemble the Bloch equations for the magnetization vector and the relaxation times T_1 and T_2 are given as the reciprocal diagonal components of the relaxation matrix.

Following the formulation described above, the present work adopts and generalizes this approach based on the quantum kinetic equations[71] to the problem of spin decoherence in a QD; the detailed mathematical derivation is provided in the Appendix. As the kinetic equations under discussion [see Eq. (A15) as well for details] do not assume specific properties of the heat bath H_L (except a short τ_c) nor the interaction mechanism H_{SL}, they form the backbone of our theoretical approach. Note, however, that use of the first Born approximation excludes from consideration the higher-order interactions such as the two-phonon processes of Fig. 2(b) (which appear on the second order of H_{SL}). In the following sections, we show how they can be applied to the specific cases of QD spin decoherence, particularly the elastic processes corresponding to anharmonic vibration and "local-field steps" in Table I. It amounts to the evaluation of the Fourier-transformed correlation function as discussed in the Appendix [see $\pi\gamma_{zz}^0$ of Eq. (A18)].

IV. ANHARMONIC VIBRATIONS

There are several manifestations of the elastic relaxation process termed "anharmonic vibration." To avoid difficulties in determining adequate mechanisms of spin-phonon interaction and their interference, we consider this problem semi-phenomenologically by applying the parameters of the spin-deformation Hamiltonian,[70] which can be extracted from the electron paramagnetic resonance (EPR) experiments on shallow donors in strained crystals or known dependencies of electron g-tensor shift in a low-symmetry potential. These parameters are mainly associated with simultaneous manifestation of direct modulation of spin-orbit interaction and the admixture mechanism as discussed above (see Table II). We also take into account the hyperfine interaction (HFI) modulation mechanism when the spin-deformation Hamiltonian is not applicable. A brief preliminary account of this process was given earlier.[34]

A. Qualitative analysis

Our analysis is based on the representation of spin-phonon interaction in terms of fluctuating effective magnetic field $\mathbf{\Omega}$ (in units of energy) acting on the electron spin **s**. This field is assumed to be composed of additive contributions $\mathbf{\Omega}_p$ from each phonon $p=\{\mathbf{q},\varkappa\}$ with a wave vector **q** and polarization $\varkappa$, i.e., $\mathbf{\Omega}=\Sigma_p \mathbf{\Omega}_p$. For the moment, let us focus on a single-phonon contribution. Then, in the frame of reference rotating with a Zeeman frequency, the electron spin performs precession around the small $\mathbf{\Omega}_p$, which oscillates with the phonon frequency ω_p. No alteration in the electron-spin phase occurs due to such a harmonic perturbation, with a possible exception of spin phase shift $\Delta\phi_0$ acquired at the initial period of interaction $0<t<2\pi/\omega_p$ due to a random phonon phase θ_p.[72]

A different situation can be realized when the phonon harmonic oscillation is interrupted and resumes at a series of instant times t_{1i} and t_{2i} $(i=1,2,\ldots)$, respectively, as shown in Fig. 3. The reason for such phonon fluctuations can be lattice anharmonicity, phonon scattering at the impurities or lattice defects, etc. These irregular phonon perturbations affect the electron-spin precession, resulting in the phase shift $\Delta\phi_i$ at each interval of time $t_{2i}-t_{1i}$. Subsequently, the net effect of spin phase change $\phi_p(t)$ due to a phonon mode p can be expressed as $\phi_p(t)=\Sigma_i \Delta\phi_i$ $(t_{2i}<t)$.

Note that for a large number of small changes $\Delta\phi_i$, their total effect can be described by a diffusion equation. Its solution leads to an exponential decay of electron-spin phase with a relaxation rate $T_p^{-1}=\frac{1}{2}\langle \Delta\phi_i^2 \rangle \tau_p^{-1}$, where τ_p is the mean time between sequential instants t_{1i} (or t_{2i}).[71] To estimate the spin phase change $\Delta\phi_i$ caused by a phonon perturbation during $t_{2i}-t_{1i}$, it is helpful to recognize that the oscillator does not change the spin phase during its full period $\Delta t_p=2\pi/\omega_p$ as well as for any n integer periods $n2\pi/\omega_p$. Hence, $\Delta\phi_i$ can be approximated as a spin rotation $\Omega_p \Delta t_p$ in an effective field $\mathbf{\Omega}_p$ independently of the duration $t_{2i}-t_{1i}$. With the mean value $\langle \Delta\phi_i \rangle$ on the order of Ω_p/ω_p, one can expect $T_p^{-1} \sim \tau_p^{-1}\Omega_p^2/\omega_p^2$ for the phonon mode p and $T_2^{-1} \sim \Sigma_p N_p \tau_p^{-1} \Omega_p^2/\omega_p^2$ when the contributions of all phonons (with the population factor N_p) are taken into account.

B. Theoretical model

The qualitative consideration provided above shows that electron-spin phase relaxation can be strongly affected by the phonon phase damping of any origin such as phonon decay. Since this mechanism does not involve energy exchange, only the longitudinal (with respect to the external magnetic field **B**) component Ω_z of the effective fluctuating field is relevant to our case. Since the random single-spin fluctuation associated with each phonon scattering is expected to be very small, we investigate the total result of these small fluctuations averaged over the time scale Δt $(\tau_c \ll \Delta t \ll T_2)$. Thus, the time evolution of the mean spin value **s** can be described in terms of the quantum kinetic equation discussed in Sec. III and in the Appendix [see Eqs. (A15) and (A18)].[71] As mentioned earlier, the analysis of $T_{2,0}^{-1}=\pi\gamma_{zz}^0$ is the focus of the investigation since it determines the transversal relaxation stemming from the elastic processes.

The z component of the fluctuating field operator due to the phonon decay can be expressed in a form linear in the creation and annihilation operators $a_p^\dagger$ and a_p of the phonon mode $p=\{\mathbf{q},\varkappa\}$ ($\mathbf{q}$ and $\varkappa$ are the phonon wave vector and its polarization, $-p\equiv\{-\mathbf{q},\varkappa\}$); i.e.,

$$\Omega_z = \sum_p V_z^p Q_p, \tag{3}$$

$$Q_p = a_p^{\dagger} - a_{-p}, \tag{4}$$

with a matrix element V_z^p of the spin-phonon interaction whose specific form will be discussed later. Skipping the detailed elaboration of the routine calculation of the phonon correlation functions,[73,74] the final result for the spin-relaxation rate associated with the elastic anharmonic vibration process is obtained as

$$T_{2,0}^{-1} = \sum_p |V_z^p|^2(2N_p+1)\frac{\tau_p^{-1}}{\omega_p^2}, \tag{5}$$

where τ_p is the phonon relaxation time (see Ref. 75 and references therein) and the phonon population factor N_p is given as $[\exp(\hbar\omega_p/k_BT)-1]^{-1}$. This expression is in accordance with the qualitative analysis discussed in the previous section with the exception of the second term in the factor $2N_p+1$ (i.e., "1") that is attributed to the zero-point vibrations. It reflects the quantum effects, which could not be described in terms of a classical approach but may be important at low temperatures.

To evaluate Eq. (5), one needs the knowledge of the relevant phonon mode p (such as the dispersion relation ω_p and the relaxation time τ_p) as well as its interaction with electron spins. Taking into account the conditions frequently adopted in QC, we assume that the radius of the electronic state a_0 (i.e., the QD size) is much larger than the lattice constant. This restricts the summation in Eq. (5) to long-wavelength phonons as the matrix element V_z^p falls off quickly for $q > \pi/a_0$. Accordingly, $\tau_p=\tau_\varkappa(\mathbf{q})$ can be considered in the long-wavelength limit. Following the analysis of Ref. 76 [see Eq. 6.2 therein], the complex functional dependence of τ_p on the temperature and phonon frequencies can be expressed as $\tau_p^{-1}=\tau_{bs}^{-1}+I_s\omega_p^4+P_sq^4+(N_s+U_s)q^2T^3$. Here, τ_{bs}^{-1} accounts for the boundary scattering that is independent of the phonon quantum number and the temperature,[75] parameters I_s and P_s describe the phonon scattering at the isotopes and point defect strain fields, and N_s and U_s represent the normal and umklapp processes of the phonon-phonon scattering. It is clear from the form of the expression that only one term τ_{bs}^{-1} survives in the long-wavelength limit and at sufficiently low temperatures $T \lesssim T_{bs}$ ($T_{bs}\approx 10$ K in the case of Ref. 76). Since this mechanism is insensitive to p and T as mentioned earlier, it is adequate to assume a constant phonon relaxation time $\tau_p \simeq \tau_{ph}$. The simple relaxation time approximation circumvents the difficult problem of the zone-edge phonons and the dependence $\tau_p=\tau_\varkappa(\mathbf{q})$, which could be very specific for each particular sample.

C. Effect of acoustic modes

To evaluate Eq. (5) (i.e., $|V_z^p|^2$) for the acoustic phonons, we consider a phenomenological Hamiltonian of the spin-lattice interaction. It can be expressed in terms only of symmetry and does not depend on a specific mechanism;[70]

$$H_{SL}^{ac} = \sum_{ijkl} A_{ijkl}\mu_B B_i s_j \overline{u_{kl}} + \sum_{ijklm} A'_{ijklm}\mu_B B_i s_j \overline{w_{klm}}. \tag{6}$$

Here $\overline{u_{kl}}$ is the strain tensor $u_{kl}=(\partial\Delta x_k/\partial x_l+\partial\Delta x_l/\partial x_k)/2$ averaged over the electron ground state $|g\rangle$ (i.e., $\overline{u_{kl}} =\langle g|u_{kl}|g\rangle$), subscripts $ijkl$ refer to the crystallographic axes, and the nonzero components of the tensor A_{ijkl} can be found from the symmetry of the QD.[18,70] The second term in Eq. (6) takes into account the effect of strain gradient $w_{klm} =\partial u_{kl}/\partial x_m$, which will be neglected from consideration since it can be irrelevant to the elastic spin-phonon processes.[19]

As a specific problem, we consider a lateral [001] QD with a z-directed magnetic field and a localized electron with the axial symmetry with respect to the z axis. This case can be applied to high-symmetry systems corresponding, for example, to shallow donors, Now, Eq. (6) can be reduced to the form $H_{SL}^{ac}=\mathbf{\Omega s}$ with $\Omega_z=[(A_{33}-A_{31})\overline{u_{zz}}+A_{31}\overline{\Delta}]\mu B$ and $\Omega_x =\Omega_y=0$.[18] Δ denotes the dilatation $\Delta=\Sigma_i u_{ii}$ and the Voigt notation is adopted ($A_{33}=A_{zzzz}$, $A_{31}=A_{zzxx}$, and $A_{66}=A_{xyxy}$). Then, as Ω_z is expressed in terms of the creation and annihilation operators [Eq. (3)], the matrix element V_z^p is given as

$$V_z^p = i\left(\frac{\hbar}{2\rho V_0\omega_p}\right)^{1/2}[(A_{33}-A_{31})e_z^p q_z + \delta_{\varkappa,L}A_{31}q]\Phi(\mathbf{q})\mu_B B. \tag{7}$$

Here, ρ is the mass density of the crystal, $q=\sqrt{q_x^2+q_y^2+q_z^2}$, V_0 is the volume of the sample structure, $\mathbf{e}^p$ the polarization vector of the phonon p, and $\Phi(\mathbf{q})=\langle g|e^{i\mathbf{q}\cdot\mathbf{r}}|g\rangle$.

The spin-lattice relaxation rate in Eq. (5) can be calculated by treating the acoustic-phonon modes based on the isotropic elastic continuum model with the longitudinal and transverse sound velocities v_L and v_T. Then by taking advantage of the phonon relaxation time approximation (in the long-wavelength limit and at sufficiently low temperatures) as well as the axial symmetry for the localized electron [i.e., $\Phi(\mathbf{q})=\Phi(x,z)$ with $x=qa_0/2$, $z=q_z/q$], one can obtain

$$T_{2,0}^{-1} = \tau_{ph}^{-1}\xi(B)\int_0^\infty x\sum_{\varkappa=L,T}\frac{v_T^3}{v_\varkappa^3}\coth\left(\frac{T_\varkappa^{eff}}{T}x\right)F_\varkappa(x)dx,$$

$$\xi(B) = \frac{(A_{33}-A_{31})^2\mu_B^2B^2}{2\pi^2\hbar\rho v_T^3a_0^2},$$

$$F_\varkappa(x) = \int_{-1}^{1} P_\varkappa(z)(z^2+\zeta)^2\Phi^2(x,z)dz, \tag{8}$$

where we introduce $1/a_0^2$ and a_0^2 into $\xi(B)$ and integrate for convenience. In this equation, $P_L(z)=(z^2+\zeta)^2$, $P_T(z)=z^2(1-z^2)$, τ_{ph}^{-1} is the average phonon relaxation rate as mentioned above, $T_\kappa^{eff}=\hbar v_\varkappa/k_Ba_0$ is the effective temperature, and $\zeta \equiv A_{31}/(A_{33}-A_{31})=-1/3$ if one assumes that the strain-induced part of the effective g-tensor $\tilde{g}_{ij}=\Sigma_{k,l}A_{ijkl}u_{kl}$ is characterized by zero trace, i.e., $A_{33}+2A_{31}=0$.

1. Spin decoherence of shallow donor

Let us evaluate spin relaxation of a shallow donor electron with an effective Bohr radius $a_B(=a_0)$ and $\Phi(x,z)=(1+x^2)^{-2}$. The last factor determines the relevant phonons, which must be long-wavelength modes with $q\lesssim 1/a_B$. Then, the integral in Eq. (8) has a simple analytical approximation,

$$T_{2,0}^{-1}=\frac{2\xi(B)\tau_{ph}^{-1}}{45}\left(\sqrt{1+\frac{T^2}{T_T^2}}+\frac{2v_T^3}{3v_L^3}\sqrt{1+\frac{T^2}{T_L^2}}\right), \tag{9}$$

where $T_{L(T)}=(16/15\pi)T_{L(T)}^{eff}$; this result is for the case of $\mathbf{B}\parallel[001]$.

As an example, we consider a phosphorus shallow donor in Si with $a_B=1.8$ nm. The phonon relaxation time can be extracted from the low-temperature measurements of Si thermal resistivity[77] in terms of the theory developed in Refs. 75 and 78 ($\tau_{ph}=2.4\times10^{-8}$ s). The spin-phonon coupling constants were estimated in Refs. 79 and 80. However, we believe that direct determination of coupling constants by means of EPR measurements of Si:P under an applied stress gives more reliable data. A corresponding experiment was performed in Ref. 81, where the constant $A_{66}=0.44$ was found. Similarly, our estimation[34] obtains $A_{33}=0.31$ and $A_{31}=-0.155$ that gives $T_{2,0}^{-1}=1.3\times10^{-4}$ s^{-1} at the magnetic field of 1 T and low temperatures $T\ll T_{L(T)}\simeq10$ K. In another important case of a Si shallow donor in Al$_{0.4}$Ga$_{0.6}$As, the data on EPR under a uniaxial stress[82] provide rather strong spin-phonon constants of $A_{33}=19.6$ and $A_{31}=-9.8$. This gives the estimations $T_{2,0}^{-1}=6.1\times10^{-2}$ and 6.1×10^{-4} s^{-1} for the magnetic fields of 1 and 0.1 T, respectively, at $T=4$ K under the assumption that phonon lifetimes are identical in these crystals.

2. *Spin decoherence in a QD*

Corresponding calculations can be performed for an electron localized in a QD of $L_{xy}=2a_0$ in lateral width and $L_z=\epsilon L_{xy}$ in thickness. Under the condition $\epsilon\lesssim0.1$, an approximate formula takes the form

$$T_{2,0}^{-1}=\xi(B)\tau_{ph}^{-1}\left(\sum_{i=L,T}b_i\sqrt{c_i^2+d_i^2\frac{T^2}{T_i^2}}\right), \tag{10}$$

where the fitting coefficients are $b_T=1$, $b_L=v_T^3/v_L^3$, $c_T=0.33-1.27\epsilon^2$, $d_T=0.35-0.395\epsilon^2$, $c_L=0.97-28.5\epsilon^2$, and $d_L=0.40-3.76\epsilon^2$.

To examine the importance of spin phase relaxation caused by the phonon decay, the result of Eq. (10) is compared with the admixture spin-flip process[16] in a GaAs QD with $L_z=3$ nm and $L_{xy}=25$ nm, assuming $\tau_{ph}=2.4\times10^{-8}$ s and $A_{33}=19.6$. For the relatively strong magnetic field of 1 T and $T=4$ K, the present elastic process and the spin-flip give $T_{2,0}^{-1}\approx0.1$ s^{-1} and $\frac{1}{2}T_1^{-1}=T_{2,\omega}^{-1}=10$ s^{-1}, respectively, while for $B=0.1$ T, both predict almost the same rate of $\approx10^{-3}$ s^{-1}. At lower magnetic fields, the elastic spin relaxation prevails. The Si QD gives a qualitatively similar (but smaller) result; its numerical estimation will be discussed in Sec. VII.

D. Role of optical phonons

The optical phonons possess high energies compared to the typical energy scale (such as the thermal energy k_BT) and, thus, are generally ignored in the problem of QC based on QD electron spins.[83,84] However, this is not the case in the elastic process under consideration since the uncontrolled variation of spin phase can happen without the presence of thermal phonons as shown in Eq. (5) at $N_p\to0$. Zero-point optical vibrations, which survive even at very low temperatures $T\ll\hbar\omega_{op}$ (ω_{op} is the optical-phonon frequency), contribute to spin decoherence as happens with acoustic modes in the case $T\ll T_{L,T}$ [Eq. (10)]. The potential significance of the optical modes stems from their relatively large contributions at small wave vectors q [$|V_z^p|^2\to$constant as $q\to0$ (Ref. 85)] as well as the substantially shorter phonon lifetime. In contrast, $|V_z^p|^2\to q$ for acoustic phonons in the long-wavelength limit.

For a detailed analysis, consider a QD made of a polar crystal. The longitudinal-optical phonons induce the electron potential

$$\varphi_{op}=\sqrt{\frac{2\pi\hbar\omega_{op}}{V_0\tilde{\kappa}}}\sum_{\mathbf{q}}\frac{\exp(i\mathbf{qr})}{q}(a_{\mathbf{q}}^{\dagger}-a_{-\mathbf{q}}), \tag{11}$$

where $1/\tilde{\kappa}=1/\kappa_\infty-1/\kappa_0$; κ_∞ and κ_0 are the corresponding dielectric constants. Assume that the QD possesses an asymmetrical potential in the growth direction z due to an effective electric field $\mathbf{F}$ imposed along this axis (e.g., the gate bias). Since F influences the electron g tensor,[67] its superposition with φ_{op} results in a spin-phonon interaction $H_{SL}^{op}=\mu_BB(dg/dF)d\varphi_{op}/dz$ that is linear in the phonon operator. After substitution of Eq. (11), this expression reduces to the form of Eq. (3) with

$$|V_z^p|^2=\left(\mu_BB\frac{dg}{dF}\right)^2\frac{2\pi\hbar\omega_{op}}{V_0\tilde{\kappa}}\frac{q_z^2}{q^2}\Phi^2(\mathbf{q}). \tag{12}$$

Finally, the spin-relaxation rate is obtained as

$$T_{2,0}^{-1}=\tau_{op}^{-1}\xi_{op}(B), \tag{13}$$

$$\xi_{op}(B)=\frac{2}{\sqrt{\pi}\tilde{\kappa}}\frac{\left(\frac{dg}{dF}\mu_BB\right)^2}{\hbar\omega_{op}V_{QD}}, \tag{14}$$

where V_{QD} is the QD volume ($=L_{xy}^2L_z$).

The distinctive property of transversal relaxation described by Eq. (13) is its proportionality to $(dg/dF)^2$. As the sensitivity of g tensor to the external electric field is determined by its orbital contribution $g-g_0$ (the free-electron Landè factor $g_0\approx2.0023$), this relaxation mechanism is expected to be important in the compounds with strong spin-orbital coupling (such as III-V and II-VI semiconductors). As a specific example, we perform numerical estimation for a GaAs QD of $L_{xy}=50$ nm and $L_w=5$ nm. Here, evaluating the QD potential asymmetry *a priori* provides the most significant challenge. Following the calculations performed for Ga$_{0.47}$In$_{0.53}$As/InP quantum wells,[67] a typical value for $\frac{dg}{dF}$ seems to be approximately 0.085 nm/mV at $F>10$ mV/nm with $\mathbf{B}$ directed along the growth axis, while for the perpendicular direction $\frac{dg}{dF}\leqslant0.035$ nm/mV. As the effect of optical phonons quenches in the case of a symmetrical potential ($\frac{dg}{dF}=0$ with $F=0$), only the upper limit of this contribution can be estimated, i.e., $\xi_{op}(1\text{ T})\leqslant7\times10^{-6}$. Taking into account that $\tau_{op}^{-1}\simeq10^{11}$ s^{-1},[85] one can find $T_{2,0}^{-1}\leqslant C_{op}B^2$, where $C_{op}=7\times10^5$ s^{-1} T^{-2}. Thus, $T_{2,0}$ can be as short as 100 ns at $B=3.5$ T and $T=1$ K. This estimation shows that the transversal relaxation via zero-point optical vibrations can potentially be a very effective spin decoherence mechanism in asymmetrical structures, particularly made of compound semiconductors with strong spin-orbital coupling. A similar theoretical observation was made with respect to the *charge qubit* decoherence in coupled QDs,[86] where optical phonons were shown to shorten coherent states at low and even zero temperatures very efficiently.

E. Effects of hyperfine interaction and two-phonon processes

Let us consider the elastic one-phonon process associated with the modulation of hyperfine interaction as well as the two-phonon process. Since these processes result in sufficiently slow and/or long spin relaxation, we shall restrict our consideration to a brief discussion.

The Hamiltonian of hyperfine interaction with the nuclear spin $\mathbf{I}_j$ located at site j with the position $\mathbf{r}_j$ takes the form

$$H_{hf}=a_{hf}\sum_j|\psi_g(\mathbf{r}_j)|^2\mathbf{I}_j\mathbf{s}, \tag{15}$$

where $\psi_g(\mathbf{r})=|g\rangle$ is an electron wave function. The spin-phonon interaction due to small oscillations at $\mathbf{r}_j$ can be expressed in terms of the dilatation operator $\bar{\Delta}=\langle g|\Delta|g\rangle$ if the mean internuclear distance ($\approx n_I^{-1/3}$, n_I is the nuclear-spin concentration) is shorter than the wavelength of relevant phonons; i.e., $H_{SL}^{hf}=\mathbf{\Omega}\mathbf{s}$, where $\mathbf{\Omega}=\hat{n}a_{hf}\bar{\Delta}\sqrt{I(I+1)n_I/V_{QD}^{hf}}$. Here, the unit vector $\hat{n}$ is directed along the effective nuclear field defined by Eq. (15) and $V_{QD}^{hf}=(\int|\psi(\mathbf{r})|^4d^3\mathbf{r})^{-1}$. Calculation of the phase relaxation rate for the case of a shallow donor results in the following expression, which is similar to Eq. (9):

$$T_{2,0}^{-1}=\frac{\xi_{hf}\tau_{ph}^{-1}}{3}\sqrt{1+\frac{T^2}{T_L^2}}, \tag{16}$$

$$\xi_{hf}=\frac{I(I+1)n_Ia_{hf}^2}{6\pi^2\hbar\rho V_{QD}^{hf}v_L^3a_0^2}. \tag{17}$$

Similarly, one can find the approximate rate for an electron localized in a QD through an analogy with Eq. (10),

$$T_{2,0}^{-1}=\xi_{hf}\tau_{ph}^{-1}\sqrt{c_{hf}^2+d_{hf}^2\frac{T^2}{T_L^2}}, \tag{18}$$

where $c_{hf}=3.7-68\epsilon^2$, $d_{hf}=2.7-9.8\epsilon^2$, and $\epsilon\lesssim 0.1$. Numerical estimations provided for a donor in Si and GaAs in terms of Eq. (16) indicate inefficiency of this mechanism with a very long relaxation time (about 10^{14} and 10^8 s, respectively). Hence, this mechanism can be neglected in most cases.

Along with the Hamiltonian given in Eq. (6), the spin–two-phonon interaction $H_{SL}^{(2)}=\Sigma D_{ijklmn}\mu_BB_is_ju_{kl}u_{mn}$ can also contribute to spin decoherence (D_{ijklmn} is the spin–two-phonon coupling constant). Now, the fluctuating effective field takes the form $\Omega_\alpha=\Sigma_{p,p'}W_\alpha^{p,p'}Q_pQ_{p'}$, where $W_\alpha^{p,p'}$ are the matrix elements of $H_{SL}^{(2)}$. Hence the Fourier image of the correlation function $\gamma_{\mu\nu}(\omega)$ [Eq. (A12)] is expressed in terms of phonon correlation functions $\langle(Q_{p_1}Q_{p_2})(\tau)Q_{p_3}Q_{p_4}\rangle_\omega$. Its calculation performed in a harmonic approximation leads to a simple approximation for the spin phase relaxation rate

$$T_{2,0}^{-1}=\frac{\mu_B^2B^2D^2}{21\rho^2v_T^3}\left(\frac{k_BT}{\hbar v_T}\right)^7. \tag{19}$$

The parameter D can be estimated as $D=3(g-g_0)C^2/E_g^2$; C and E_g are the deformation potential and the energy band gap. Numerical evaluation of Eq. (19) at low temperatures ($T=4$ K) predicts a long relaxation time. In the case of GaAs and $B=1$ T, one can find $T_{2,0}\approx 3\times 10^5$ s, which is too long to be of any experimental or practical interest.

V. PRECESSION FLUCTUATIONS

This section analyzes the elastic process listed as "Local-field steps" in Table I. The specific spin-phonon interactions under consideration are the indirect mechanisms resulting from g-tensor fluctuation and hyperfine field fluctuation (see Table II) via the stochastic transitions between different electronic states.

A. Qualitative consideration

Consider an electron spin $\mathbf{s}$ under the influence of a magnetic field directed along the z axis whose strength fluctuates in a stepwise fashion in time. In this case, the projection of electron spin on the z axis s_z is conserved and no longitudinal relaxation occurs. Nevertheless, the phase of electron spin will change randomly with the Zeeman frequency fluctuation $\delta\Omega$. At the scale of time $t\gg\tau_c$ (τ_c is the correlation time of the fluctuation),[71] the Markovian process can be used to describe the decoherence rate as $T_2^{-1}\sim\langle\Delta\phi^2\rangle/\tau_c$ with the mean value of the squared phase shift $\langle\Delta\phi^2\rangle$ acquired between two successive sudden changes of Ω. Taking into account that $\langle\Delta\phi^2\rangle\approx\delta\Omega^2\tau_c^2$, one can find the dependence $T_2^{-1}\sim\delta\Omega^2\tau_c$. As discussed earlier, the origin of $\delta\Omega$ can be the phonon-mediated stochastic transitions between different orbital states. Since the spin splitting characteristics vary with the orbital states, electrons experience uncontrollable changes in the precession frequency (thus, the phase) while undergoing spin-independent phonon scattering between them. In the case of a QD, this process may play an important role owing to the shallow energy levels and the dependence of g tensor or hyperfine constant on the electronic orbital states.[36]

B. Theoretical model

We begin the quantitative analysis by defining the Hamiltonian H over the basis functions consisting of a few lowest electronic states $|n\rangle$, which are involved due to the phonon-assisted transitions. We also consider that the single-electron problem in the QD gives a doubly degenerate energy spectrum E_n with the eigenstates $|n\rangle$ in the absence of the Zeeman energy and the hyperfine interaction. When a magnetic field is applied, it is conveniently assumed that the differences in the spin splitting of the electronic states $|n\rangle$ and $|n'\rangle$ are small with respect to the energy intervals $|E_n-E_{n'}|$. The specific nature and type of the QD is unimportant for the analysis.

With these conditions, the total Hamiltonian can be expressed as

$$H = H_s + H_e + H_{ph} + H_{e\text{-}ph}. \tag{20}$$

The first term H_s is the spin (or pseudospin) energy Hamiltonian which can be reduced to the form $H_s=\hat{\mathbf{\Omega}}\mathbf{s}$ in the most general case with $\hat{\Omega}_z=\langle\uparrow|H_s|\uparrow\rangle-\langle\downarrow|H_s|\downarrow\rangle$ as discussed in Eq. (2). Its projection on the lowest electronic states $|n\rangle$ reads (see, for comparison, Refs. 79 and 80)

$$\hat{\mathbf{\Omega}} = \sum_{n,n'} |n\rangle \mathbf{\Omega}^{n,n'} \langle n'|, \tag{21}$$

where $\mathbf{\Omega}^{n,n'}$ are the matrix elements of the effective field (in units of energy) taken between the $|n\rangle$ and $|n'\rangle$ states. The spin-independent (i.e., orbital) electron energies describe the Hamiltonian H_e

$$H_e = \sum_n E_n |n\rangle\langle n|. \tag{22}$$

The Hamiltonians of the lattice and electron-phonon interactions have the usual form

$$H_{ph} = \sum_p \omega_p \left(a_p^+ a_p + \frac{1}{2} \right), \tag{23}$$

$$H_{e\text{-}ph} = \sum_{p,n,n'} B^p_{n,n'} |n\rangle\langle n'| (a_p^+ + a_{-p}). \tag{24}$$

Here, $B^p_{k,k'}$ is the matrix element of the electron-phonon interaction that depends on the material parameters and the geometry of the QD. The last three terms of Eq. (20) constitute the Hamiltonian of the dissipative subsystem $H_L(=H_e+H_{ph}+H_{e\text{-}ph})$ following the notation of Eq. (2).

Thus, the problem of spin relaxation is reduced to calculating the correlation functions of the effective-field operator with the Hamiltonian H_L of the dissipative subsystem. Clearly, the derivation depends strongly on the specific form of H_L, the energy spectrum, and the quantity of electron states considered. Keeping this context in mind, we consider the simpler problem of electron fluctuations between only two discrete states $|n\rangle=|g\rangle$ or $|e\rangle$ that are the ground and first excited electronic energy states (with an energy separation of δ_0). The corresponding Zeeman frequencies are denoted $\Omega_z^{(g)}$ $[=\Omega_z^{g,g}$ in Eq. (21)] and $\Omega_z^{(e)}$ $(=\Omega_z^{e,e})$, respectively. Such a simplification allows us to easily perform all the necessary calculations in an analytical form. In addition, most of the important physics of the mechanism under consideration can be obtained in the framework of this two-level model.

Hereinafter, it is convenient to introduce Pauli matrices σ_1, σ_2, and σ_3 on the basis $|e\rangle$, $|g\rangle$, where, according to the definition, σ_1, σ_2, and σ_3 are invariant with respect to the coordinate system rotation in contrast to actual spin matrices $\mathbf{s}$. Then, the Hamiltonian of the dissipative subsystem takes the form

$$H_L = H_{ph} + \frac{1}{2}\delta_0\sigma_3 + \sum_p B_p \sigma_1 (a_p^+ + a_{-p}). \tag{25}$$

The electron-spin Hamiltonian H_s can now be split into the steady part H_S and fluctuating component H_{SL} with

$$H_S = \frac{1}{2}(\mathbf{\Omega}^e + \mathbf{\Omega}^g)\mathbf{s}\hat{\mathbf{1}} \tag{26}$$

and

$$H_{SL} = \frac{1}{2}(\mathbf{\Omega}^{(e)} - \mathbf{\Omega}^{(g)})\mathbf{s}\sigma_3, \tag{27}$$

where $\hat{\mathbf{1}}$ represents the unity matrix in the basis $|e\rangle$, $|g\rangle$. According to Eq. (A5), we must find $V=H_{SL}-\langle H_{SL}\rangle=\mathbf{\Omega}\mathbf{s}$ from Eq. (27) that determines $\mathbf{\Omega}=\frac{1}{2}(\mathbf{\Omega}^{(e)}-\mathbf{\Omega}^{(g)})(\sigma_3-\langle\sigma_3\rangle)$ with $\langle\sigma_3\rangle=-\tanh(\delta_0/2k_BT)$. The correlation functions in Eq. (A12) now take the form

$$\gamma_{\mu\nu}(\omega) = \frac{1}{4}(\Omega_\mu^{(e)} - \Omega_\mu^{(g)})(\Omega_\nu^{(e)} - \Omega_\nu^{(g)}) J_\omega(T), \tag{28}$$

$$J_\omega(T) = \langle (\sigma_3(\tau) - \langle\sigma_3\rangle)(\sigma_3 - \langle\sigma_3\rangle)\rangle_\omega. \tag{29}$$

The function $J_\omega(T)$ can be obtained by using the double-time Green's function $G(t,t')=\langle\langle\sigma_3(t);\sigma_3(t')\rangle\rangle$ with H_L. The final expression takes the following form:[36]

$$J_\omega(T) = \frac{1-\langle\sigma_3\rangle^2}{\pi n(\omega)} \frac{\tau_c}{\omega^2\tau_c^2 + 1}, \tag{30}$$

$$\tau_c^{-1} = 2\pi \sum_p |B_p|^2 \langle Q_p(\tau) Q_{-p}\rangle_{\delta'}, \tag{31}$$

where the difference between $\delta'=\delta_0-\frac{1}{2}(\Omega_z^{(e)}-\Omega_z^{(g)})$ and δ_0 will be ignored in the subsequent consideration. In the harmonic approximation, one can find

$$\langle Q_p(\tau) Q_{-p}\rangle_{\delta'} = (2N_p + 1)\delta(\omega_p - \delta_0), \tag{32}$$

with the phonon population factor $N_p=\langle a_p^+ a_p\rangle$ for mode p. τ_c takes the simple physical meaning of the correlation time caused by phonon-assisted transitions between the $|g\rangle$ and $|e\rangle$ states.

C. Temperature dependence of phase relaxation

Actually, Eqs. (28)–(32) describe the problem under consideration in a very general form. As a result, an analysis on the temperature dependence can be provided even before the details of the phonon-mediated mechanism that induces the effective-field fluctuation are determined. Specifically, the correlation time τ_c given in Eq. (31) can be written as $\tau_\delta \tanh(\delta_0/2k_BT)$ with the aid of Eq. (32), where $\tau_\delta=[2\pi\Sigma_p|B_p|^2\delta(\omega_p-\delta_0)]^{-1}$ is the lifetime of the excited electron state with respect to the transition to the ground state through phonon emission in the limit $T\to 0$. Thus, for the $\omega=0$ component (e.g., γ_{zz}^0), the temperature dependence of spin relaxation is reduced to

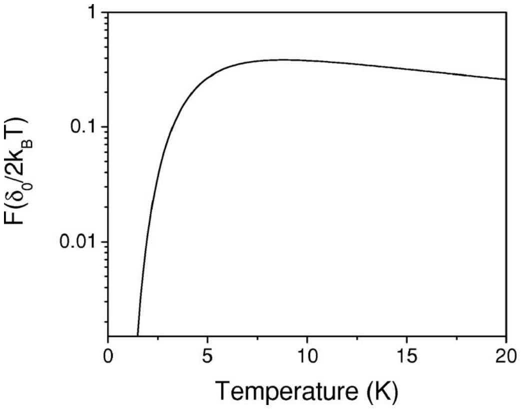

FIG. 4. Decoherence factor $F(\delta_0/2k_BT)$ [i.e., Eq. (33)] for the process of precession fluctuation as a function of temperature assuming $\delta_0=1$ meV.

$$J_0(T)=\frac{\tau_\delta}{\pi}F\left(\frac{\delta_0}{2k_BT}\right),\quad F(x)=(1-\tanh^2 x)\tanh x. \quad (33)$$

Figure 4 shows the numerical evaluation of $J_0(T)$ as a function of T assuming $\delta_0=1$ meV. A maximum is observed at a temperature near $k_BT=\delta_0$, with distinctive slopes on each side. The left of the peak corresponds to the reduced hopping from the $|g\rangle$ to $|e\rangle$ state that decreases the difference $\mathbf{\Omega}^{(g)}-\langle\mathbf{\Omega}^{(g)}\rangle$ (or the amplitude of fluctuations). Hence, in the limit $T\ll\delta_0$, the effective-field fluctuations are frozen and our mechanism becomes ineffective as $F(\delta_0/2k_BT)\to\exp(-\delta_0/k_BT)$. The slow negative slope on the high-temperature side [i.e., $F(\delta_0/2k_BT)\to\delta_0/2k_BT$] arises due to the well-known effect of dynamical fluctuation averaging, which becomes more pronounced with an increase in temperature.

D. Effect of *g*-tensor fluctuation

The general theory discussed above is applied to a specific mechanism of phase relaxation, which stems from the hopping between the excited and ground states with different g tensors. In the most general case, the reason for such a difference is the g-tensor dependence on the energy separation between the discrete electronic levels and the nearest spin-orbital split electronic band. For technologically significant III-V compounds, where the interaction with the valence-band edge determines the deviation of electron g tensor from g_0 ($\approx$2.0023),[87] one can find the amplitude of the fluctuation $\Delta g=(dg/dE_g)\delta_0$ with $dg/dE_g=(g_0-g)(\Delta_{so}+2E_g)/E_g(\Delta_{so}+E_g)$, where E_g is the band gap and Δ_{so} the spin-orbital splitting of the valence band; we also assume the inequality $\delta_0\ll E_g$. In the case of a Si QD, E_g is a splitting of the Δ point in the Brillouin zone.[79] Then, the final equation for the phonon-assisted rate of phase relaxation caused by the fluctuations of Zeeman splitting is given by

$$T_{2,Z}^{-1}=\frac{(g_0-g)^2}{4g^2}\left[\frac{\delta_0(\Delta_{so}+2E_g)}{E_g(\Delta_{so}+E_g)}\right]^2\omega_0^2\tau_\delta F\left(\frac{\delta_0}{2k_BT}\right), \quad (34)$$

where $\hbar\omega_0=g\mu_BB$. One can see that our mechanism reveals a quadratic dependence of $T_{2,Z}^{-1}$ on the applied magnetic field B in contrast to the $\sim B^5$ dependence found in the previous calculations of longitudinal spin-lattice relaxation through the direct (one-phonon) processes.[16–18,79,80]

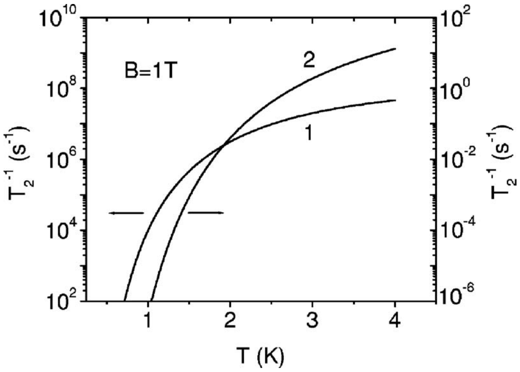

FIG. 5. Spin decoherence rate via the g-tensor fluctuation mechanism [i.e., Eq. (34)] as a function of temperature for $\delta_0=1$ meV and $B=1$ T. Curve 1 is for a GaAs QD, while curve 2 considers a Si QD with $g_0-g_\parallel=0.0131$ and $g_0-g_\perp=0.0141$.

An estimation of the excited-state lifetime τ_δ can be performed in terms of a deformation potential interaction and a model of lateral carrier confinement. The matrix element of the corresponding electron-phonon interaction between the $|g\rangle$ and $|e\rangle$ states is provided in Ref. 18 as $B_q=iC\sqrt{\hbar q/2\rho v_LV_0}J_{osc}$, where $J_{osc}=J_{osc}(\mathbf{q})$ is a form factor, V_0 is the volume of the crystal, and C, ρ, and v_L are the deformation potential, mass density, and longitudinal sound velocity as defined earlier. A straightforward calculation of inverse lifetime results in the expression

$$\tau_\delta^{-1}=\frac{C^2q_\delta^3\alpha}{32\pi^2\hbar\rho v_L^2}\int_0^1(1-z^2)e^{-\alpha(1-z^2)}dz, \quad (35)$$

where $q_\delta=\delta_0/\hbar v_L$, $\alpha=\delta_0/2m_ev_L^2$, and m_e is the lateral effective mass.

To show the efficiency of the mechanism under consideration, we calculate the relaxation rates in terms of Eqs. (34) and (35) for a GaAs QD with $\delta_0=1$ meV and the magnetic field $B=1$ T as a function of temperature (Fig. 5, curve 1). A similar calculation is provided for a Si QD with $g_0-g_\parallel=0.0131$ and $g_0-g_\perp=0.0141$ (Ref. 81) (Fig. 5, curve 2). A comparison between the result of Fig. 5 and the T_1 calculation[18,19] shows that the phonon-induced g-tensor fluctuation via excited states can control the phase relaxation in a Si QD at $T\gtrsim 2$ K (i.e., $T_{2,Z}<T_1$) in spite of a small g_0-g (see Sec. VII for a detailed quantitative analysis); in the case of a GaAs QD, this elastic process prevails over the spin-flip transitions at $T\gtrsim 1$ K and $B\lesssim 1$ T.

E. Effect of nuclear field fluctuation

A similar fluctuation arises in the nuclear hyperfine field when the electron undergoes uncontrollable transitions between the orbital $|e\rangle$ and $|g\rangle$ states. As shown in Eq. (15), the hyperfine interaction is influenced by the electronic envelope functions evaluated at the location of the nuclear spins. Hence, the difference in $\Psi_e(\mathbf{r})$ and $\Psi_g(\mathbf{r})$ leads to a dispersion of the hyperfine field whose mean value is given as

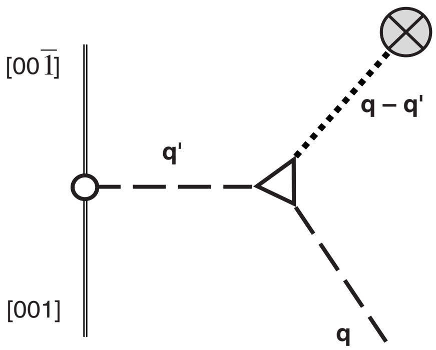

FIG. 6. Diagram of the phonon-mediated intervalley relaxation process in a crystal with inhomogeneous deformations. The [001] and [00$\bar{1}$] denote the electron states in the two equivalent valleys; the circle represents the electron-phonon matrix element, the triangle depicts third-order anharmonicity, and the crossed circle is for the point defect. The real phonon $\mathbf{q}$ splits into two virtual phonons $\mathbf{q}'$ and $\mathbf{q}-\mathbf{q}'$ due to the lattice anharmonicity. The latter is accommodated by the local deformation of the point defect that can be of short wavelength with $|\mathbf{q}'| \gg |\mathbf{q}|$. Consequently, the other virtual phonon can have a momentum $\mathbf{q}'$ large enough to induce the intervalley transition.

$\delta\Omega_n = a_{hf}\sqrt{\frac{2}{3}I(I+1)\varkappa_0 n_I/V_{QD}}$. Here, I and n_I are the nuclear spin and its concentration in a QD of volume V_{QD} as discussed before; the dimensionless parameter $\varkappa_0 = V_{QD}\int(|\Psi_e(\mathbf{r})|^2 - |\Psi_g(\mathbf{r})|^2)^2 d^3\mathbf{r}$ is equal to $9/16\pi$ within the approximations of Ref. 18. If we set $\Omega_z^{(e)} - \Omega_z^{(g)} = \delta\Omega_n$ in Eq. (28), we readily find the following estimation:

$$T_{2,hf}^{-1} = \frac{\varkappa_0}{6} I(I+1) \frac{a_{hf}^2 n_I}{V_{QD}} \tau_\delta F\left(\frac{\delta_0}{2k_B T}\right). \qquad (36)$$

This equation shows the independence of spin relaxation ($T_{2,hf}$) on the magnetic field when the process is induced by the hyperfine interaction. An estimation of Eq. (36) (with an appropriate averaging[88] over ^{69}GA, ^{71}Ga, and ^{75}As) for a GaAs QD with a typical size of $L_{xy}=50$ nm, $L_z=5$ nm, and $\delta_0=1$ meV gives $T_{2,hf}=8\times 10^{-5}$, 2×10^{-7}, and 1.7×10^{-8} s for $T=1$, 2, and 4 K, respectively. A similar estimation performed for a Si QD with the same dimensions and temperatures results in $T_{2,hf}=29$, 9×10^{-2}, and 6.5×10^{-3} s, respectively. Clearly, Eq. (36) can provide a dominant contribution for spin relaxation at low fields as it does not depend on the applied magnetic field. In the case of the Si QD, a detailed quantitative analysis is provided in Sec. VII.

VI. INTERVALLEY TRANSITIONS

In this section, we consider one particular but important case that is applicable to the semiconductors with multiple equivalent energy minima. The basic principle is the same as that discussed in the previous section, i.e., via the phonon-mediated stochastic transitions. The difference is that the present case takes into account the intervalley transitions between the so-called valley-split states. Although normally prohibited, these processes become possible in the presence of point defects. Of the two potential mechanisms, the hyperfine field fluctuation is suppressed due to the equivalence of the involved valleys. However, the "g-tensor fluctuation" mechanism maintains its significance as the degeneracy of these states is lifted (i.e., valley split with different energies) in asymmetrical structures.

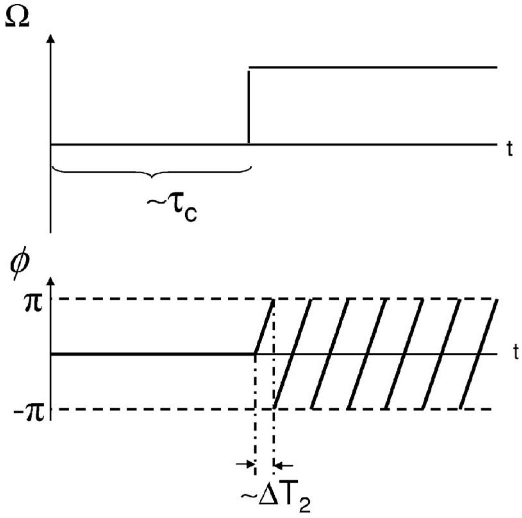

FIG. 7. Schematic illustration of phase relaxation in the case of inequality $T_2 \ll \tau_c$, where T_2 is the transversal relaxation time in the Markovian kinetic equations. In time of approximately τ_c, the effective field is subject to a sudden large change. This causes relatively fast spin phase diffusion with the time scale of ΔT_2. Hence, the duration of the two-step process, $\approx \tau_c$, can be associated with the phase relaxation time.

A. Qualitative consideration

Following the brief discussion given above, this mechanism can occur in semiconductors with multiple equivalent energy minima. As a specific example, a QD grown along the [001] (i.e., z) direction with six equivalent minima near the X point is considered (i.e., Si-like); the cases with different crystallographic symmetries can be analyzed with a similar treatment. Subsequently, the valley-orbital structure of the QD assumes the ground state formed by two equivalent valleys [001] and [00$\bar{1}$] with the wave functions ψ_{001} and $\psi_{00\bar{1}}$. Any center-asymmetrical potential $V(r)$ (with respect to the z direction) removes the degeneracy over the equivalent valleys with a valley-orbital splitting $\Delta E_{v\text{-}v}$, thus forming the even and odd states $\psi_\pm = (\psi_{001} \pm \psi_{00\bar{1}})/\sqrt{2}$. In the case of a triangular potential $V(r)$, an estimation predicts the splitting of $\Delta E_{v\text{-}v} = l_{v\text{-}v} dV(r)/dz$ with $l_{v\text{-}v} \approx 0.5$ Å in Si.[89] Clearly, one can see that a moderately asymmetrical confinement potential can result in an energy splitting sufficiently large to induce the g-tensor fluctuation under an appropriate lifetime τ_δ. However, the phonon-induced transitions between the valley-orbital states with a different parity are normally forbidden or sufficiently suppressed.[90]

This restriction is lifted when one considers a structure composed of solid solutions. For example, the Ge atoms in a $\mathrm{Si}_{1-x}\mathrm{Ge}_x$ QD with $x \ll 1$ (that offers a promising candidate for

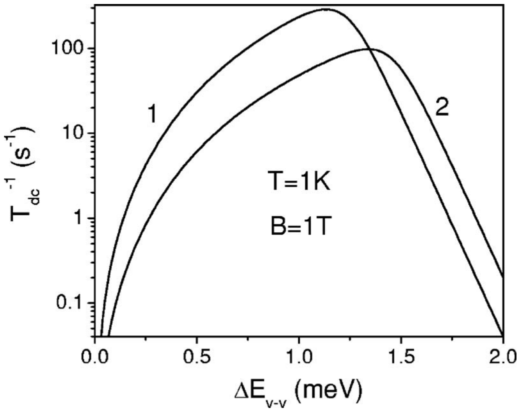

FIG. 8. Spin decoherence rate via the intervalley transitions as a function of valley-orbital splitting. Curve 1 is for $Si_{0.9}Ge_{0.1}$ (namely, the defect density of 10%), while $Si_{0.98}Ge_{0.02}$ is considered for curve 2.

solid-state[91] QC) can be treated as the point defects in the Si lattice. The phonon scattering with point defects due to the lattice anharmonicity results in the appearance of high-frequency harmonics that can transfer electrons between the equivalent valleys [001] and $[00\bar{1}]$ or between the valley-orbital states with a different parity. Figure 6 presents a diagram of the process responsible for these transitions. As schematically illustrated, the third-order anharmonicity splits a phonon resonant with $\Delta E_{v\text{-}v}$ into two high-frequency virtual phonons. One of them is "frozen" due to the static deformation surrounding the defect, while the other phonon induces the electron to undergo an intervalley scattering. The transfer between the states with an energy separation leads to the fluctuation in the electron precession frequency as described in the previous section.

B. Analysis of intervalley transition

The estimation of spin decoherence rate due to the transitions between the valley-split states can be performed in terms of Eq. (34) when the lifetime τ_δ is calculated taking into account the valley-orbital structure of a QD. However, direct application of Eq. (32) to Eq. (31) would result in vanishingly small matrix elements B_q with $\hbar\omega_q = \Delta E_{v\text{-}v}$ for the case of intervalley transitions. In order to take into consideration the process depicted in Fig. 6, one must supplement the Hamiltonian [Eq. (23)] with terms accounting for the phonon scattering at the defects:[76]

$$H_3 = \sum_{q,q'} F_{q,q',q'-q} Q_q Q_{q'}, \tag{37}$$

$$F_{q,q',q'-q} = \frac{\hbar}{2\rho V_0}\frac{C_{q,q'}}{\sqrt{\omega_q \omega_{q'}}}, \tag{38}$$

where the matrix element of phonon scattering is

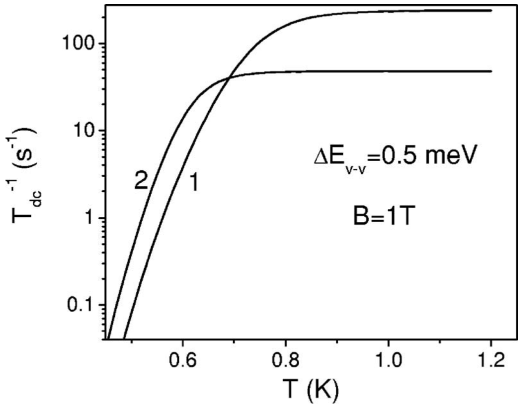

FIG. 9. Spin decoherence rate via the intervalley transitions as a function of temperature. Curve 1 is for $Si_{0.9}Ge_{0.1}$, while $Si_{0.98}Ge_{0.02}$ is considered for curve 2.

$$C_{q,q'} = i\frac{g_c}{2a^3}\sum_{\mathbf{a}} (\mathbf{V}_{q'-q}\mathbf{a})(\mathbf{e}_q\mathbf{a})(\mathbf{e}_{q'}\mathbf{a})(\mathbf{q}\mathbf{a})(\mathbf{q}'\mathbf{a})[(\mathbf{q}-\mathbf{q}')\mathbf{a}]. \tag{39}$$

Here, g_c is a constant, **a** the unit vectors connecting neighboring lattice atoms, and $\mathbf{V}_q$ a Fourier transformation of the static displacement $\mathbf{y}(\mathbf{r})$ caused by point defects. Additionally, a more general expression is applied for the correlation function (see, for example, Refs. 73 and 74) in place of Eq. (32), which is obtained in a harmonic approximation:

$$\langle Q_p(\tau)Q_{-p}\rangle_\omega = \frac{1}{\pi}\frac{(2N_p+1)\Gamma_p(\omega)}{(\omega^2-\omega_p^2)^2/\omega_p^2+\Gamma_p^2(\omega)}. \tag{40}$$

The phonon damping rate $\Gamma_p(\omega)$ must be calculated in terms of the interaction specified by Eqs. (37)–(39). Following the works of Refs. 74 and 92, it is given as

$$\Gamma_p(\omega) = 8\pi\sum_{q'} |F_{p,p',p'-p}|^2[\delta(\omega-\omega_{p'})-\delta(\omega+\omega_{p'})] \tag{41}$$

in terms of the Hamiltonian $H_{ph}+H_3$ [Eqs. (23) and (37)].

For simplicity, we ignore the lattice anisotropy and consider the displacement $\mathbf{y}(\mathbf{r})$ in the model of isotropic medium:[76,92]

$$\mathbf{y}(\mathbf{r}) = \sum_{j=1}^{N_D} A_D \frac{\mathbf{r}-\mathbf{R}_j}{|\mathbf{r}-\mathbf{R}_j|^3}, \tag{42}$$

where A_D is a mismatch in the lattice volume between the host and substitutional impurity atoms. As it plays the role of deformation charge, this parameter (i.e., A_D) can be found from the analysis of EPR linewidth.[93] The Coulombic deformation field resulting from Eq. (42) gives a well-known expression

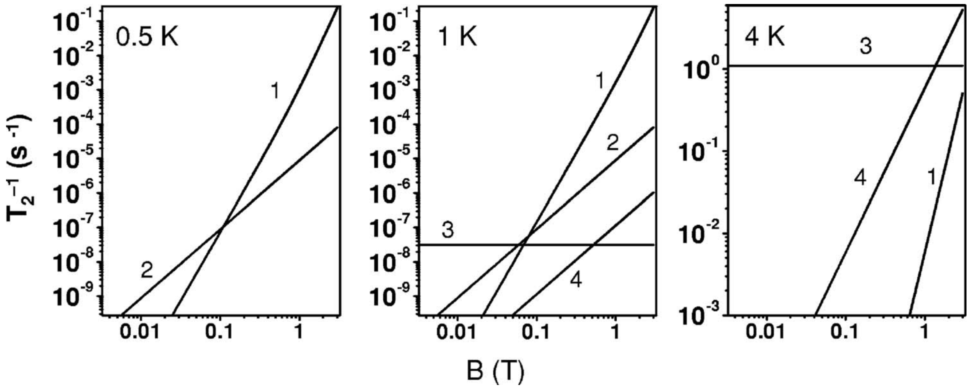

FIG. 10. Spin decoherence rate vs magnetic field for the dominant spin-phonon relaxation processes in a typical Si QD (of $5\times 50\times 50$ nm^3): line 1, inelastic direct spin-flip process; line 2, elastic process of acoustic-phonon anharmonic vibration; line 3, elastic process of local-field steps due to the hyperfine field fluctuation; and line 4, elastic process of local-field steps due to the g-tensor fluctuation. The temperatures are as shown in the figure; the energy splitting δ_0 between the ground and excited states is fixed at 2 meV. Since a Si QD is assumed without any point defects, the process via the intervalley transition is not considered.

$$\mathbf{V}_q = 4\pi i \frac{A_D}{V_0}\sum_{j=1}^{N_D} e^{i\mathbf{q}\mathbf{R}_j}\frac{\mathbf{q}}{q^2}. \tag{43}$$

Then, substitution of Eqs. (38), (39), and (43) into Eq. (41) and follow-up integration over the phonon spectrum in the Debye model (i.e., $\omega_p \equiv \omega_{q,\varkappa} = v_\varkappa q$) result in

$$\Gamma_{\varkappa,q}(\omega) = \frac{27\pi}{16} n_D \Sigma_\varkappa \frac{A_D^2 g_c^2}{\rho^2 v_L^7}\omega^3\omega_q, \tag{44}$$

where n_D is the concentration of point defects. The coefficient $\Sigma_\varkappa$ in this equation takes into account the contributions of the phonon modes with different polarizations. In the approximation of an isotropic medium, one can find $\Sigma_L = S_{LL} + (v_L/v_T)^2 S_{LT}$, where the sums $S_{\kappa\kappa'} = \langle\{\Sigma_{\hat{a}}(\mathbf{e}_{\mathbf{q}}^{\kappa}\hat{a})(\mathbf{e}_{\mathbf{q}}^{\kappa'}\hat{a})(\hat{q}\hat{a}) \times (\hat{q}'\hat{a})[(\hat{q}-\hat{q}')\hat{a}]^2\}^2\rangle_{(4\pi)^2}$ account for the polarization mixing; $\hat{a} = \mathbf{a}/a$; $\hat{q} = \mathbf{q}/q$; and $\langle\cdots\rangle_{(4\pi)^2}$ means averaging over the directions of $\mathbf{q}$ and $\mathbf{q}'$. A numerical estimation for the diamond lattice gives $S_{LL} = 0.789$ and $S_{LT} = 0.239$; hence, $\Sigma_L = 1.29$ for Si. Finally, the Fourier transformation of the correlation function [Eq. (40)] is obtained as

$$\langle Q_p(\tau)Q_{-p}\rangle_\omega = \frac{27}{16\hbar}(2N_p+1) n_D \Sigma_\varkappa \frac{A_D^2 g_c^2}{\rho^2 v_L^7}\frac{\omega^3}{\omega_q} \tag{45}$$

for the phonons connecting the equivalent valleys.

The next step is to evaluate the matrix element of the intervalley electron-phonon interaction [see Eq. (31)]. It assumes the form

$$B_p = \sqrt{\frac{\hbar}{2\rho V_0 \omega_p}}\left(\Xi_d + \frac{1}{3}\Xi_u\right) q\,\delta_{\varkappa,L}\Phi(\mathbf{q}), \tag{46}$$

where Ξ_d and Ξ_u are the deformation potential constants and the form factor $\Phi(\mathbf{q}) = \langle\psi_\mp|e^{i\mathbf{q}r}|\psi_\pm\rangle$ selects the wave vectors close to the k-space separation Δk_v of the two minima. Assuming a QD with the lateral and transversal dimensions of L_{xy} and L_z, one can obtain

$$\Phi(\mathbf{q}) \approx \exp\left[-\frac{L_{xy}^2}{4}(q_x^2+q_y^2) - \frac{L_z^2}{4}(q_z+\Delta k_v)^2\right]. \tag{47}$$

The appropriate Δk_v takes the value of $\approx 0.3\pi/a_L$ (a_L the lattice constant) considering the umklapp process. Substitution of Eqs. (44) and (46) into Eq. (40) results in the contributions of two different types. The first is a direct process and, as mentioned earlier, has only a minor significance to τ_c with a characteristic factor $\sim\exp\left[-\frac{L_z^2}{2}\Delta k_v^2\right] \ll 1$. On the other hand, the second type accounts for the electron interaction with virtual phonons of energy $\omega_q \gg \Delta E_{v\text{-}v}$. This contribution is calculated with the help of Eqs. (45)–(47):

$$\tau_c = \tau_\delta \tanh\frac{\Delta E_{v\text{-}v}}{2k_B T}, \tag{48}$$

$$\tau_\delta^{-1} = C_{iv} n_D \gamma^2 \frac{A_D^2 \Xi^2 \Delta E_{v\text{-}v}^3}{\hbar^4 \rho V_{QD} v_L^5}. \tag{49}$$

When deriving Eq. (48), an estimation $g_c = 24\gamma\rho\bar{c}^2$ from Ref. 76 is used that defines the constant $C_{iv} \simeq 210$.

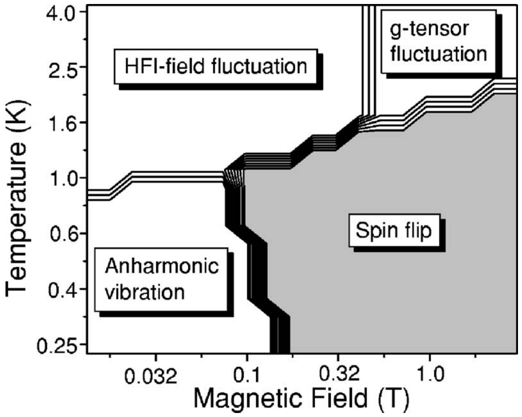

FIG. 11. Diagram of dominant spin-relaxation processes in the Si QD in the B-T parameter space. The same conditions as in Fig. 10 are assumed (for example, $\delta_0 = 2$ meV). The unshaded region is where the elastic spin-phonon processes dominate.

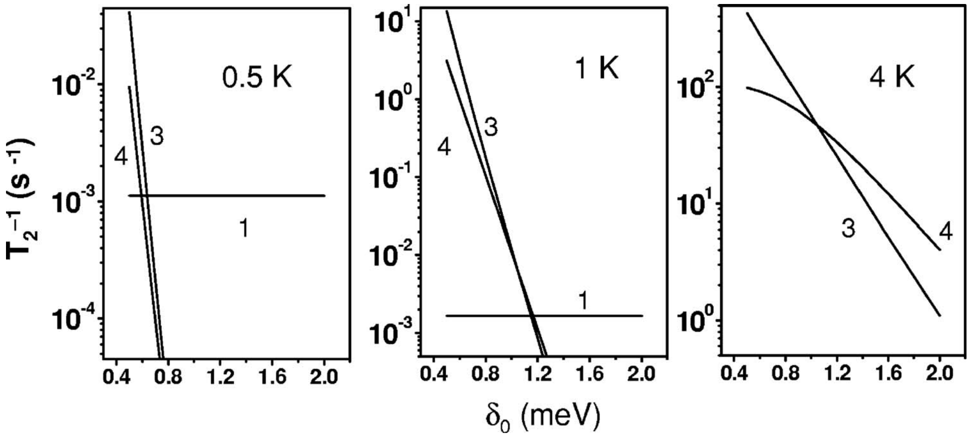

FIG. 12. Spin decoherence rate vs δ_0 for the dominant spin-phonon relaxation processes in a typical Si QD (of $5\times50\times50$ nm^3): line 1, inelastic direct spin-flip process; line 3, elastic process of local-field steps due to the hyperfine field fluctuation; and line 4, elastic process of local-field steps due to the g-tensor fluctuation. The temperatures are as shown in the figure; the magnetic field is fixed at 1 T. Since a Si QD is assumed without any point defects, the process via the intervalley transition is not considered.

C. Spin decoherence due to intervalley transitions

With the intervalley transition mediated by the point defects as described above, we can now calculate the subsequent spin relaxation due to the associated fluctuation in the local magnetic field. Evidently, the hyperfine interaction does not take part in the process since the equivalent valley-orbital states possess identical electronic envelope functions. Hence, only the g-tensor fluctuations due to the valley-split energy is considered. As in Sec. V, applying Eq. (48) to Eq. (34) solves the problem under the condition $\tau_c \ll T_2$. However, it should be noted that the formal calculation of T_2 using these equations violates the required inequality condition when $\Delta E_{v\text{-}v}$ is sufficiently small. Subsequently, the Markovian kinetic equations [Eqs. (A17)–(A19)] are unsuitable. Actually the spin decoherence time can be determined by τ_c itself in the regime, where the result for $T_{2,Z}$ [see Eq. (34)] is much shorter than τ_c, as schematically illustrated in Fig. 7. Here, the spin relaxation can be considered in two stages. The first is the "pending" period of approximately τ_c, during which the electron has not undergone the intervalley scattering. Obviously, no change occurs in the electron-spin phase. Once the transition is made, the electron is subject to the effective magnetic field (due to the difference in the g tensor) and starts to acquire the phase change. Within a typical time on the order of $\Delta T_2 \simeq \hbar / |\Omega^{(e)} - \Omega^{(g)}|$ ($\ll \tau_c$), the electron fully loses the information regarding the initial state. The intermediate case $T_2 \approx \tau_c$ remains beyond the quantitative consideration. For simplicity, we apply an interpolation $T_{dc} \approx T_2 + \tau_c$. The calculated decoherence time T_{dc} for a Si$_{1-x}$Ge$_x$ QD is plotted as a function of $\Delta E_{v\text{-}v}$ (Fig. 8) and temperature (Fig. 9). Two cases of Ge composition ($x=0.1$ and $x=0.02$) are considered assuming the QD size of $L_{xy}=50$ nm and $L_z=5$ nm. Clearly, the proposed mechanism can significantly increase the spin relaxation rate in the mixed crystals. Even with the smaller "defect" concentration of 2%, T_{dc} can be reduced to the 10 ms range. Particularly, this rate is very strongly dependent on the magnitude of the splitting $\Delta E_{v\text{-}v}$ (in reference to the thermal energy). Hence, the control of the valley splitting will be essential for long coherence. For estimation, we assume $\Xi=8.6$ eV, $\rho=2.33$ g/cm^3, $v_L=8.43\times10^5$ cm/s, $\gamma=0.56$,[75] and $C_{iv}\approx 210$. The deformation charge A_D was found to be 1.2×10^{-25} cm^3 for a Ge atom[94] in Si from Ref. 93.

VII. COMPARISON BETWEEN DIFFERENT MECHANISMS

To gauge the significance of the elastic processes, the relevant transversal spin-relaxation rates (T_2^{-1}) are obtained numerically in a Si QD (with $5\times50\times50$ nm^3) as a function of temperature, magnetic field, and orbital energy separation. In addition to the three elastic processes described in this paper (i.e., anharmonic vibration and local-field steps due to the g-tensor fluctuation and hyperfine field fluctuation), the contribution by the direct spin flip (that is, the dominant inelastic process in Si) is taken into account for comparison.[18] Since Si is not a mixed crystal and the defect density kept low for the QC application, the process via the intervalley transition is not considered. Figure 10 shows the calculated T_2^{-1} vs B when the energy separation δ_0 is fixed at 2 meV. For the range of temperatures considered in the study, it is apparent from the result that the direct spin-flip dominates at a sufficiently high magnetic field ($\gtrsim 1$ T) due to its strong dependence (e.g., $B^4 - B^5$). For low fields, the anharmonic vibration (i.e., acoustic-phonon decay) process tends to be significant particularly when the temperature is also low. As the temperature increases, the contributions due to the local-field steps become prominent. While the g-tensor fluctuation mechanism plays a greater role at a stronger B, the field-independent nature of the nuclear field makes it stand out in the other extreme. The corresponding map of the dominant process and/or mechanism in the B-T parameter space ($\delta_0=2$ meV) is given in Fig. 11, clearly signifying the importance of elastic relaxation.

A similar comparison is provided in Fig. 12 as a function of the orbital energy separation δ_0 at three different temperatures. The magnetic field is set to 1 T. Note that the contribution due to the anharmonic vibration process is not shown

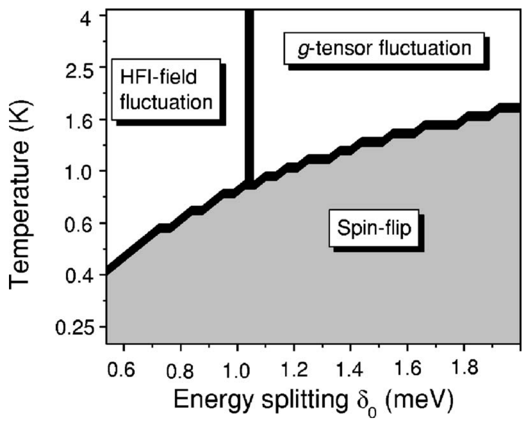

FIG. 13. Diagram of dominant spin-relaxation processes in the Si QD in the δ_0-T parameter space. The same conditions as in Fig. 12 are assumed (for example, $B=1$ T). The unshaded region is where the elastic spin-phonon processes dominate.

as its relaxation rate falls below the range of presentation. From the figure, it is clear that the relaxation induced by the local-field steps (via both the g-tensor and hyperfine field fluctuation mechanisms) is very sensitive to δ_0; this can be readily understood as the process requires round-trip transitions by overcoming δ_0. Subsequently, its contribution is important only for a small δ_0 (in reference to $k_B T$). Since the spin-flip rate is practically independent of δ_0 and T in the considered parameter range, the crossover point between these rates monotonically moves to a higher δ_0 with increasing T. At 4 K, the inelastic process drops out of the picture. Of the two elastic mechanisms, the g-tensor case seems to be relatively more efficient as δ_0 increases. This may be due to the fact that the change in the g tensor is directly proportional to the orbital energy separation. Figure 13 summarizes the dominant process and/or mechanism identified in the δ_0 $-T$ parameter space at $B=1$ T. Considering the conditions typical for QC using an electron spin in a Si QD (e.g., $\delta_0 \lesssim 1$ meV, $T \lesssim 1$ K, and $B \gtrsim 1$ T), it is expected that T_2 over 10 s can be achieved. If a SiGe QD is used in place of Si, then the decoherence process can become more active depending on the valley-split energy. However, T_2 on the order of 10 ms or longer is still attainable. The spin relaxation in a GaAs QD is predicted to be much faster.

Table III summarizes the functional dependence of the dominant relaxation processes considered in this study. The zeroth power (e.g., T^0, B^0, δ_0^0) denotes the independent nature of the corresponding parameter. The unique set of T, B, and δ_0 dependences will facilitate the experimental identification of each process. As the thermal energy provides the unwanted error and/or noise, the parameter space relevant to QC is where T is much smaller than the other characteristic energies.

VIII. CONCLUSION

A group of elastic spin-relaxation processes that do not involve the energy exchange between the Zeeman subsystem and the thermal reservoir is studied in semiconductor QDs. Contrary to common perception, these processes can play a dominant role in the electron-spin decoherence under certain conditions (magnetic field, temperature, orbital energy separation, etc.) as identified in the investigation. Particularly, the calculation results illustrate the potential significance of an elastic decoherence mechanism originating from the intervalley transitions in semiconductor quantum dots with multiple equivalent energy minima (e.g., the X valleys in SiGe). The detailed understanding obtained in this work will help in optimizing the QD-based QC systems for long quantum coherence; for example, the Si-based QDs can offer a spin-relaxation time that is much longer than the GaAs counterparts. However, an additional, comprehensive effort is needed for a complete analysis of spin decoherence, taking into account all the possible contributions and their manifestations.

ACKNOWLEDGMENTS

This work was supported in part by the Defense Advanced Research Projects Agency and the SRC/MARCO Center on FENA.

APPENDIX: DERIVATION OF BASIC EQUATIONS FOR ELECTRON-SPIN EVOLUTION

For a detailed description, we start with the kinetic equation for the spin-density matrix

TABLE III. Functional dependence of the dominant spin-phonon processes on the relevant parameters considered in this study. The zeroth power (e.g., T^0, B^0, δ_0^0) denotes the independent nature of the corresponding parameter. The temperature T, magnetic field B, and Zeeman frequency ω are expressed in units of energy. T^* stands for a characteristic temperature, based on which the low- and high-temperature regimes are defined. Eqs refer to the corresponding equations given in the text.

		Temperature			Magnetic field		Energy separation	
Process	Eqs	$T\ll$	T^*	$\ll T$	$T \ll \omega$	$T \gg \omega$	$T \ll \delta_0$	$T \gg \delta_0$
Direct spin flip		T^0	ω	T^1	B^5	B^4		
Anharmonic vibration	10	T^0	T_{eff}	T^1	B^2	B^2	δ_0^0	δ_0^0
g-tensor steps	34	$e^{-\delta_0/T}$	δ_0	T^{-1}	B^2	B^2	$e^{-\delta_0/T}$	δ_0
HF field steps	36	$e^{-\delta_0/T}$	δ_0	T^{-1}	B^0	B^0	$\delta_0^2 e^{-\delta_0/T}$	δ_0^{-1}

$$\hat{\sigma} = \mathrm{Tr}_L \rho, \tag{A1}$$

with the Hamiltonian as given in Eq. (2). Here, ρ obeys the Liouville equation $i\rho = \widetilde{H}\rho$, where the sign "$\sim$" over any operator A means the Liouville superoperator: $\widetilde{A}B = [A,B] = AB - BA$. The trace Tr_L is taken over all variables of the system except the given electron spin, and $\hbar$ and k_B are set to 1 in this section. Assuming that the thermal bath is in a thermodynamic equilibrium, one can introduce its statistical operator

$$f_L = \frac{\exp(-\beta H_L)}{\mathrm{Tr}_L \exp(-\beta H_L)}, \quad \beta = \frac{1}{T}. \tag{A2}$$

Following the approach developed in Ref. 95 with a projection operator method (see Ref. 96), the kinetic equation of the operator $\hat{\sigma}$ in the Born approximation is obtained as

$$\frac{d\hat{\sigma}(t)}{dt} = -i\widetilde{H}_S\hat{\sigma}(t) - \mathrm{Tr}_L\left\{ \widetilde{V}(t)\int_0^t \widetilde{V}(t,t') f_L \widetilde{S}_d(t,t')\hat{\sigma}(t')dt' \right\}, \tag{A3}$$

where

$$S_d(t,t') = \exp\left\{ -i\int_{t'}^{t} \widetilde{H}_S(\tau)d\tau \right\},$$

$$\widetilde{V}(t,t') = S_d(t,t')\widetilde{V}(t)S_d^{-1}(t,t'),$$

$$\widetilde{V}(t) = \exp\{i\widetilde{H}_L(t)\}\widetilde{V}\exp\{-i\widetilde{H}_L(t)\}.$$

The collision integral in Eq. (A3) involves the electron-spin states at instants t' preceding the current time t; thus it is not yet a Markovian equation. The Markovian approximation corresponds to the first step of iteration that yields $\hat{\sigma}(t') = S_d^{-1}(t,t')\hat{\sigma}(t)$ in Eq. (A3). In terms of the ordinary operators, it takes the form

$$\frac{d\hat{\sigma}(t)}{dt} = -i[H_S,\hat{\sigma}(t)] - \int_0^t \mathrm{Tr}_L[V(t,t),[V(t,t'),f_L\hat{\sigma}(t)]]dt'. \tag{A4}$$

Equation (A4) implies renormalization of the spin-bath interaction

$$V = (\mathbf{\Omega}^{(g)} - \langle \mathbf{\Omega}^{(g)} \rangle)\mathbf{s}, \tag{A5}$$

so that the averaging over the bath $\langle \cdots \rangle = \mathrm{Tr}_L f_L \ldots$ results in $\langle V \rangle = 0$, while $H_S = H_S^{(g)} + \langle \mathbf{\Omega}^{(g)} \rangle \mathbf{s}$. In the case of time-independent H_S, the operators on the right-hand side of Eq. (A4) take the forms

$$V(t,t') = \exp\{-iH_S(t-t')\}V(t')\exp\{iH_S(t-t')\}, \tag{A6}$$

$$V(t) = \exp(iH_L t)V\exp(-iH_L t). \tag{A7}$$

Although the integrand in Eq. (A4) can be calculated for arbitrary coordinates, its subsequent application is not very convenient. Without the loss of generality, the z axis can be chosen along the quantization direction that reduces the spin Hamiltonian to

$$H_S = \omega s_z. \tag{A8}$$

Note that the z axis, generally speaking, does not coincide with the direction of the external magnetic field if the g tensor reflects the low symmetry of a QD and $\omega = \sqrt{\Sigma_i (g_i \mu_B B_i + \langle \Omega_i^{(g)} \rangle)^2} \equiv g_{eff}\mu_B B$. Here, g_i are the principal values of g tensor, while B_i and $\Omega_i^{(g)}$ are the vector components along the main axes of g tensor.[97] By adopting the specified coordinate system, Eqs. (A6) and (A7) can be easily calculated with $\Omega_\mu = \Omega_\mu^{(g)} - \langle \Omega_\mu^{(g)} \rangle$,

$$V(t,t') = \Omega_x(t')(s_x \cos u + s_y \sin u) + \Omega_y(t')(s_y \cos u - s_x \sin u) + \Omega_z(t')s_z, \tag{A9}$$

$$V(t) = \Omega_x(t)s_x + \Omega_y(t)s_y + \Omega_z(t)s_z, \tag{A10}$$

where $u = \omega(t-t')$ and $\Omega_\mu(t)$ is defined similar to Eq. (A7). One can see that the collision integral can be expressed in terms of double-time correlation functions

$$\langle \Omega_\mu(t), \Omega_\nu(t') \rangle = \mathrm{Tr}_L\{e^{-\beta H_L}\Omega_\mu(t), \Omega_\nu(t')\} \tag{A11}$$

with an evident property $\langle \Omega_\mu(t), \Omega_\nu(t') \rangle = \langle \Omega_\mu(t-t'), \Omega_\nu(0) \rangle = \langle \Omega_\mu(0), \Omega_\nu(t'-t) \rangle$. We consider that these correlation functions reduce to zero as soon as $|t-t'|$ exceeds the correlation time τ_c. Thus, two regimes of spin evolution must be distinguished.[98] In the first regime for short times $t \ll \tau_c$, the relaxation coefficients in Eq. (A4) are proportional to t. This leads to a quadratic-on-t deviation from the initial states of the system that reproduces the very general results obtained previously in various analysis (see Refs. 99 and 100). Such a nonlinearity results in only a marginal effect of spin transition from the ground state at sufficiently short times (Zeno effect[101]). Consequently, we focus on the second, opposite case of reasonably long time $t \gg \tau_c$, when the upper limit of the integral in Eq. (A4) can tend to infinity, $t \to \infty$. In this case, the relaxation coefficients are independent of time and Eq. (A4) describes the Markovian process with exponential evolution of $\hat{\sigma}(t)$.

To proceed further, it is convenient to introduce the Fourier transformation of the correlation functions [Eq. (A11)],

$$\gamma_{\mu\nu}(\omega) = \frac{1}{2\pi}\int_{-\infty}^{\infty} \langle \Omega_\mu(\tau), \Omega_\nu(0) \rangle e^{i\omega\tau} d\tau. \tag{A12}$$

Considering the functional form of Eq. (A4), another useful relation is

$$\int_0^\infty \langle \Omega_\mu(\tau), \Omega_\nu(0) \rangle e^{i\omega\tau} d\tau = \pi\gamma_{\mu\nu}(\omega) + iP\int_{-\infty}^{\infty} \frac{\gamma_{\mu\nu}(\omega')}{\omega - \omega'} d\omega', \tag{A13}$$

where we use the symbolic identity $\int_0^\infty e^{i\omega\tau}d\tau = \pi\delta(\omega) + iP\frac{1}{\omega}$; P denotes the principal value of the integral. Finally, let us express the density matrix $\hat{\sigma}(t)$ in terms of mean values $\langle s_x \rangle \equiv \mathrm{X}$, $\langle s_y \rangle \equiv \mathrm{Y}$, and $\langle s_z \rangle \equiv \mathrm{Z}$,

$$\hat{\sigma}(t) = \frac{1}{2}[\hat{1} + 4(Xs_x + Ys_y + Zs_z)], \tag{A14}$$

so that $\mathrm{Tr}_s\, \hat{\sigma}(t)s_\mu = \langle s_\mu \rangle$, where $\hat{\sigma}(t)$ is taken from Eq. (A14); $\hat{1}$ is the 2×2 identity matrix and the trace Tr_s is taken over spin states. Multiplying Eq. (A4) sequentially by s_x, s_y, and s_z from the right and taking Tr_s, one can obtain kinetic equations for $\mathbf{S} = \{X, Y, Z\}$, which define the spin vector evolution on the Bloch sphere in the most general form

$$\frac{d}{dt}\mathbf{S} = \vec{\omega} \times \mathbf{S} - \mathbf{\Gamma}(\mathbf{S} - \mathbf{S}_0). \tag{A15}$$

In this equation, $\vec{\omega} = \{0, 0, \omega\}$ is an effective magnetic field (in energy units) directed along the spin quantization axis z [see Eq. (A8)]; the 3×3 matrix Γ represents a rather complicated expression, $\mathbf{S}_0 = \{0, 0, Z_0\}$, and $Z_0 = -\frac{1}{2}\tanh\frac{\beta\omega}{2}$ is a static spin polarization due to the spin splitting ω.

The matrix Γ can be simplified notably if one takes into account the symmetry properties of the Fourier transformation of correlation functions [Eq. (A12)],[102]

$$\langle \Omega_\mu(\tau), \Omega_\nu \rangle_\omega = e^{\beta\omega} \langle \Omega_\nu(\tau), \Omega_\mu \rangle_{-\omega} = e^{\beta\omega} \langle \Omega_\nu, \Omega_\mu(\tau) \rangle_\omega. \tag{A16}$$

At the same time, only the symmetrical part $\bar{\Gamma} = \|(\Gamma_{\mu\nu} + \Gamma_{\nu\mu})/2\|$ is relevant to spin relaxation. This is because the asymmetrical part $\Delta\Gamma$ ($\Gamma = \bar{\Gamma} + \Delta\Gamma$) contributes to Eq. (A15) as an additional effective magnetic field that cannot reduce the length of vector $\Delta\mathbf{S} = \mathbf{S} - \mathbf{S}_0$: $d\Delta\mathbf{S}/dt = \frac{\Delta\mathbf{S}}{\Delta \mathrm{S}}\frac{d\Delta\mathbf{S}}{dt} = \frac{\Delta\mathbf{S}}{\Delta\mathrm{S}}[(\vec{\omega} - \overrightarrow{\Delta\omega}) \times \Delta\mathbf{S}] - \frac{\Delta\mathbf{S}}{\Delta\mathrm{S}}\bar{\Gamma}\Delta\mathbf{S} = -\frac{\Delta\mathbf{S}}{\Delta\mathrm{S}}\bar{\Gamma}\Delta\mathbf{S}$; $\Delta\omega_x = -\Delta\Gamma_{yz}$, etc. Subsequently, the contribution of $\Delta\Gamma$ to spin relaxation is ignored. We also neglect in the calculation the second term on the right-hand side of Eq. (A13) (proportional to iP) since it plays an insignificant role as well.[95,103,104] The final result of the symbolic computation for the matrix Γ reads

$$\bar{\Gamma} = \pi \begin{pmatrix} \gamma_{zz}^0 + n(\bar{\gamma}_{yy} + \tilde{\gamma}_{xy}) & -n\bar{\gamma}_{xy} & -\frac{n}{2}(\bar{\gamma}_{xz} - \tilde{\gamma}_{yz}) - \frac{1}{2}\gamma_{xz}^0 \\ -n\bar{\gamma}_{xy} & \gamma_{zz}^0 + n(\bar{\gamma}_{xx} + \tilde{\gamma}_{xy}) & -\frac{n}{2}(\bar{\gamma}_{yz} - \tilde{\gamma}_{zx}) - \frac{1}{2}\gamma_{yz}^0 \\ -\frac{n}{2}(\bar{\gamma}_{xz} - \tilde{\gamma}_{yz}) - \frac{1}{2}\gamma_{xz}^0 & -\frac{n}{2}(\bar{\gamma}_{yz} - \tilde{\gamma}_{zx}) - \frac{1}{2}\gamma_{yz}^0 & n(\bar{\gamma}_{xx} + \bar{\gamma}_{yy}) + 2n\tilde{\gamma}_{xy} \end{pmatrix}, \tag{A17}$$

where $n = n(\omega) = (1 + e^{-\beta\omega})/2$, $\bar{\gamma}_{\mu\nu} = [\gamma_{\mu\nu}(\omega) + \gamma_{\nu\mu}(\omega)]/2$, $\tilde{\gamma}_{\mu\nu} = i[\gamma_{\mu\nu}(\omega) - \gamma_{\nu\mu}(\omega)]/2$, and $\gamma_{\mu,\nu}^0 = \gamma_{\mu\nu}(0)$.[105] The spectral properties of Eq. (A16) with respect to the definition of $n(\omega)$ reveal that the relaxation matrix given in Eq. (A17) is an even function of electron-spin splitting [i.e., $\Gamma(\omega) = \Gamma(-\omega)$], as also follows from the time inversion symmetry.[106]

If the correlation functions possess some supplementary symmetry, Eq. (A17) allows further simplification. Assuming $\gamma_{\mu\nu}(\omega) = \gamma_{\nu\mu}(\omega)$, one can find

$$\bar{\Gamma} = \pi \begin{pmatrix} \gamma_{zz}^0 + n\bar{\gamma}_{yy} & -n\bar{\gamma}_{xy} & -\frac{n}{2}\bar{\gamma}_{xz} - \frac{1}{2}\gamma_{xz}^0 \\ -n\bar{\gamma}_{xy} & \gamma_{zz}^0 + n\bar{\gamma}_{xx} & -\frac{n}{2}\bar{\gamma}_{yz} - \frac{1}{2}\gamma_{yz}^0 \\ -\frac{n}{2}\bar{\gamma}_{xz} - \frac{1}{2}\gamma_{xz}^0 & -\frac{n}{2}\bar{\gamma}_{yz} - \frac{1}{2}\gamma_{yz}^0 & n(\bar{\gamma}_{xx} + \bar{\gamma}_{yy}) \end{pmatrix}, \tag{A18}$$

which readily transforms to the relaxation matrix obtained in Ref. 107. In other cases with $\gamma_{\mu\nu}(\omega) = -\gamma_{\nu\mu}(\omega)$ for $\mu \neq \nu$, Eq. (A17) can be put in a simpler form

$$\bar{\Gamma} = \pi \begin{pmatrix} \gamma_{zz}^0 + n(\bar{\gamma}_{yy} + \tilde{\gamma}_{xy}) & 0 & \frac{n}{2}\tilde{\gamma}_{yz} \\ 0 & \gamma_{zz}^0 + n(\bar{\gamma}_{xx} + \tilde{\gamma}_{xy}) & \frac{n}{2}\tilde{\gamma}_{zx} \\ \frac{n}{2}\tilde{\gamma}_{yz} & \frac{n}{2}\tilde{\gamma}_{zx} & n(\bar{\gamma}_{xx} + \bar{\gamma}_{yy}) + 2n\tilde{\gamma}_{xy} \end{pmatrix}. \tag{A19}$$

Note that Eq. (A18) is, generally speaking, derived for the case of anisotropic medium and arbitrary electron-spin splitting ω. For an isotropic medium with $\gamma_{xx}(\omega)=\gamma_{yy}(\omega)$, Eq. (A18) can be reduced to the common Bloch equations if one sets $T_1^{-1}=\pi n[\gamma_{xx}(\omega)+\gamma_{yy}(\omega)]$ and $T_2^{-1}=\pi\gamma_{zz}(0)+T_1^{-1}/2$ and omits the off-diagonal components of Γ. Many earlier studies discussed in Sec. II further suppose that $\gamma_{zz}(0)$ is negligible compared to $\gamma_{xx}(\omega)$; thus, the simple relation $T_2^{-1}=T_1^{-1}/2$ has been applied for the estimation of transversal spin relaxation. This approximation also reproduces the common expression for $T_1^{-1}=W_{\uparrow\downarrow}+W_{\downarrow\uparrow}$, where the probabilities $W_{\downarrow\uparrow}$ and $W_{\uparrow\downarrow}$ of spin-flip up and/or down transitions can be found from Fermi's golden rule. Clearly, such simplifications are not applicable in the general cases. Moreover, the spin kinetic description in terms only of two relaxation parameters T_1 and T_2 is not always tenable in anisotropic structures, as shown in Ref. 71.

[1] V. Cerletti, W. A. Coish, O. Guwat, and D. Loss, Nanotechnology **16**, R27 (2005).
[2] K. A. Valiev, Phys. Usp. **48**, 1 (2005).
[3] I. Žutić, J. Fabian, and S. Das Sarma, Rev. Mod. Phys. **76**, 323 (2004).
[4] F. X. Bronold, A. Saxena, and D. L. Smith, in *Solid State Physics*, edited by H. Ehrenreich and F. Spaepen (Academic, New York, 2004), Vol. 58.
[5] X. Hu and S. Das Sarma, Phys. Rev. Lett. **96**, 100501 (2006).
[6] P. Facchi, S. Montangero, R. Fazio, and S. Pascazio, Phys. Rev. A **71**, 060306(R) (2005).
[7] X. Marie, T. Amand, P. Le Jeune, M. Paillard, P. Renucci, L. E. Golub, V. D. Dymnikov, and E. L. Ivchenko, Phys. Rev. B **60**, 5811 (1999).
[8] Y. G. Semenov, K. N. Borysenko, and K. W. Kim, Phys. Rev. B **66**, 113302 (2002).
[9] M. M. Glazov and E. Y. Sherman, Phys. Rev. B **71**, 241312(R) (2005).
[10] I. A. Merkulov, A. L. Efros, and M. Rosen, Phys. Rev. B **65**, 205309 (2002).
[11] Y. G. Semenov and K. W. Kim, Phys. Rev. B **67**, 073301 (2003).
[12] P.-F. Braun, X. Marie, L. Lombez, B. Urbaszek, T. Amand, P. Renucci, V. K. Kalevich, K. V. Kavokin, O. Krebs, P. Voisin, and Y. Masumoto, Phys. Rev. Lett. **94**, 116601 (2005).
[13] A. M. Tyryshkin, S. A. Lyon, A. V. Astashkin, and A. M. Raitsimring, Phys. Rev. B **68**, 193207 (2003).
[14] B. Georgeot and D. L. Shepelyansky, Phys. Rev. Lett. **86**, 2890 (2001).
[15] M. S. Byrd, D. A. Lidar, L.-A. Wu, and P. Zanardi, Phys. Rev. A **71**, 052301 (2005).
[16] A. V. Khaetskii and Y. V. Nazarov, Phys. Rev. B **64**, 125316 (2001).
[17] C. Tahan, M. Friesen, and R. Joynt, Phys. Rev. B **66**, 035314 (2002).
[18] B. A. Glavin and K. W. Kim, Phys. Rev. B **68**, 045308 (2003).
[19] V. N. Golovach, A. Khaetskii, and D. Loss, Phys. Rev. Lett. **93**, 016601 (2004).
[20] V. I. Fal'ko, B. L. Altshuler, and O. Tsyplyatev, Phys. Rev. Lett. **95**, 076603 (2005).
[21] E. Y. Sherman and D. J. Lockwood, Phys. Rev. B **72**, 125340 (2005).
[22] R. Orbach, Proc. R. Soc. London, Ser. A **246**, 458 (1961).
[23] C. B. Finn, R. Orbach, and P. W. Wolf, Proc. Phys. Soc. London **77**, 261 (1961).
[24] A. V. Khaetskii and Y. V. Nazarov, Phys. Rev. B **61**, 12639 (2000).
[25] M. C. Terrile, H. Panepucci, and R. A. Cavalho, Phys. Rev. B **15**, 1110 (1977).
[26] V. Y. Zevin, V. I. Konovalov, and B. D. Shanina, Zh. Eksp. Teor. Fiz. **59**, 561 (1970) [Sov. Phys. JETP **32**, 306 (1971)].
[27] R. Hernandez and M. B. Wallker, Phys. Rev. B **4**, 3821 (1971).
[28] W. Heitler, *The Quantum Theory of Radiation* (Dover, New York, 1984).
[29] L. K. Aminov, Phys. Status Solidi B **50**, 405 (1972).
[30] A. Abragam, *The Principles of Nuclear Magnetism* (Clarendon, Oxford, 1961).
[31] S. A. Al'tshuler and B. M. Kozyrev, *Electron Paramagnetic Resonance in Compounds of Transition Elements* (Wiley, New York, 1974).
[32] R. de Sousa and S. Das Sarma, Phys. Rev. B **67**, 033301 (2003).
[33] Y. C. Cheng and R. J. Silbey, Phys. Rev. A **69**, 052325 (2004).
[34] Y. G. Semenov and K. W. Kim, Phys. Rev. B **70**, 085305 (2004).
[35] D. Mozyrsky, S. Kogan, V. N. Gorshkov, and G. P. Berman, Phys. Rev. B **65**, 245213 (2002).
[36] Y. G. Semenov and K. W. Kim, Phys. Rev. Lett. **92**, 026601 (2004).
[37] J. R. Klauder and P. W. Anderson, Phys. Rev. **125**, 912 (1962).
[38] W. B. Mims, Phys. Rev. **168**, 370 (1968).
[39] M. Chiba and A. Hirai, J. Phys. Soc. Jpn. **33**, 730 (1972).
[40] R. de Sousa and S. Das Sarma, Phys. Rev. B **68**, 115322 (2003).
[41] W. Yao, R. B. Liu, and L. J. Sham, Phys. Rev. B **74**, 195301 (2006).
[42] C. Deng and X. Hu, Phys. Rev. B **73**, 241303(R) (2006).
[43] W. M. Witzel and S. Das Sarma, Phys. Rev. B **74**, 035322 (2006).
[44] A. V. Khaetskii, D. Loss, and L. Glazman, Phys. Rev. Lett. **88**, 186802 (2002).
[45] D. Gamliel and J. H. Freed, Phys. Rev. A **39**, 3238 (1989).
[46] Y. A. Serebrennikov and U. E. Steiner, Chem. Phys. Lett. **222**, 309 (1994).
[47] Y. A. Serebrennikov, Phys. Rev. Lett. **93**, 266601 (2004).
[48] D. Pines, J. Bardeen, and C. P. Slichter, Phys. Rev. **106**, 489 (1957).
[49] V. A. Abalmassov and F. Marquardt, Phys. Rev. B **70**, 075313 (2004).
[50] I. Waller, Z. Phys. **79**, 370 (1932).
[51] I. Dzyaloshinskii, Phys. Chem. Solids **4**, 241 (1958).
[52] T. Moriya, Phys. Rev. **120**, 91 (1960).
[53] D. Scalbert, Phys. Status Solidi B **193**, 189 (1996).
[54] K. V. Kavokin, Phys. Rev. B **64**, 075305 (2001).
[55] D. V. Bulaev and D. Loss, Phys. Rev. Lett. **95**, 076805 (2005).
[56] A. F. Zinov'eva, A. V. Nenashev, and A. V. Dvurechenskiĭ, JETP Lett. **82**, 302 (2005).

[57] P. Stano and J. Fabian, Phys. Rev. B **72**, 155410 (2005).

[58] P. Stano and J. Fabian, Phys. Rev. B **74**, 045320 (2006).

[59] R. de L. Kronig, Physica (Amsterdam) **6**, 33 (1939).

[60] J. H. Van Vleck, Phys. Rev. **57**, 426 (1940).

[61] Y. A. Bychkov and E. I. Rashba, Pis'ma Zh. Eksp. Teor. Fiz. **39**, 66 (1984) [JETP Lett. **39**, 78 (1984)].

[62] M. I. D'yakonov and V. Y. Kocharovskii, Fiz. Tekh. Poluprovodn. (S.-Peterburg) **20**, 178 (1986) [Sov. Phys. Semicond. **20**, 110 (1986)].

[63] L. M. Woods, T. L. Reinecke, and Y. Lyanda-Geller, Phys. Rev. B **66**, 161318(R) (2002).

[64] S. I. Erlingsson and Y. V. Nazarov, Phys. Rev. B **66**, 155327 (2002).

[65] W. Yang and K. Chang, Phys. Rev. B **72**, 075303 (2005).

[66] A. A. Kiselev, E. L. Ivchenko, A. A. Sirenko, T. Ruf, M. Cardona, D. R. Yakovlev, W. Ossau, A. Waag, and G. Landwehr, J. Cryst. Growth **184/185**, 831 (1998).

[67] E. L. Ivchenko, A. A. Kiselev, and M. Willander, Solid State Commun. **102**, 375 (1997).

[68] A. D. Margulis and V. A. Margulis, Sov. Phys. Solid State **25**, 934 (1983).

[69] N. S. Averkiev and L. E. Golub, Phys. Rev. B **60**, 15582 (1999).

[70] N. G. Koloskova, Fiz. Tverd. Tela (Leningrad) **5**, 61 (1963) [Sov. Phys. Solid State **5**, 40 (1963)].

[71] Y. G. Semenov, Phys. Rev. B **67**, 115319 (2003).

[72] P. G. Klemens, *Solid State Physics* (Academic, New York, 1958), Vol. 7, p. 1.

[73] D. N. Zubarev, Usp. Fiz. Nauk **71**, 71 (1960) [Sov. Phys. Usp. **3**, 320 (1960)].

[74] K. N. Pathak, Phys. Rev. **139**, A1569 (1965).

[75] Y. J. Han and P. G. Klemens, Phys. Rev. B **48**, 6033 (1993).

[76] P. Carruthers, Rev. Mod. Phys. **33**, 92 (1961).

[77] C. J. Glassbrenner and G. A. Slack, Phys. Rev. **134**, A1058 (1964).

[78] J. Callaway, Phys. Rev. **113**, 1046 (1959).

[79] L. Roth, Phys. Rev. **118**, 1534 (1960).

[80] H. Hasegawa, Phys. Rev. **118**, 1523 (1960).

[81] D. K. Wilson and G. Feher, Phys. Rev. **124**, 1068 (1961).

[82] E. R. Glaser, T. A. Kennedy, B. Molnar, R. S. Sillmon, M. G. Spencer, M. Mizuta, and T. F. Kuech, Phys. Rev. B **43**, 14540 (1991).

[83] B. I. Kochelaev, Sov. Phys. JETP **37**, 171 (1960).

[84] C.-Y. Huang, Phys. Rev. **154**, 215 (1967).

[85] A. R. Bhatt, K. W. Kim, and M. A. Stroscio, J. Appl. Phys. **76**, 3905 (1994).

[86] V. N. Stavrou and X. Hu, Phys. Rev. B **72**, 075362 (2005).

[87] A. A. Kiselev, E. L. Ivchenko, and U. Rössler, Phys. Rev. B **58**, 16353 (1998).

[88] D. Paget, G. Lampel, B. Sapoval, and V. I. Safarov, Phys. Rev. B **15**, 5780 (1977).

[89] G. Grosso, G. Pastori Parravicini, and C. Piermarocchi, Phys. Rev. B **54**, 16393 (1996).

[90] V. N. Smelyanskiy, A. G. Petukhov, and V. V. Osipov, Phys. Rev. B **72**, 081304(R) (2005).

[91] R. Vrijen, E. Yablonovitch, K. Wang, H. W. Jiang, A. Balandin, V. Roychowdhury, T. Mor, and D. DiVincenzo, Phys. Rev. A **62**, 012306 (2000).

[92] M. A. Krivoglaz, *Theory of X-ray and Thermal-Neutron Scattering by Real Crystals* (Plenum, New York, 1969).

[93] V. E. Kustov, M. G. Mil'vitskii, Y. G. Semenov, B. M. Turovskii, V. I. Shakhovtsov, and V. L. Shindich, Sov. Phys. Semicond. **20**, 169 (1986).

[94] Note that the approximation of the deformation charge A as a difference of volumes per Ge and Si atoms in the corresponding crystals leads to an overestimation $A \simeq 3 \times 10^{-24}$ cm^3.

[95] P. N. Argyries and P. L. Kelly, Phys. Rev. **134**, A98 (1964).

[96] P. Zwanzig, J. Chem. Phys. **33**, 1338 (1960).

[97] The existence of main axes for g tensor can be proven at an arbitrarily low symmetry; see V. G. Grachev, Zh. Eksp. Teor. Fiz. **92**, 1834 (1987) [Sov. Phys. JETP **65**, 1029 (1987)].

[98] A. Sher and H. Primakoff, Phys. Rev. **119**, 178 (1960).

[99] L. A. Khalfin, JETP Lett. **8**, 65 (1968).

[100] K. Urbanowski, Phys. Rev. A **50**, 2847 (1994).

[101] B. Misra and E. C. G. Sudarshan, J. Math. Phys. **18**, 756 (1977).

[102] The sign of exponent "–" in a similar expression of Ref. 71 corresponds to the definition of Fourier transformation with sign-i in exponent.

[103] C. P. Slichter, *Principles of Magnetic Resonance* (Springer-Verlag, New York, 1992).

[104] V. Zevin, Phys. Rev. B **11**, 2447 (1975).

[105] The anisotropy of Eq. (A17) as well as the correlation between all the spin components of $\mathbf{s}$ are the main distinctions between these equations and the well-known Bloch-Redfield equations [see, for instance, K. Blum, *Density Matrix Theory and Applications* (Plenum, New York, 1996)].

[106] L. D. Landau and E. M. Lifshitz, *Electrodynamics of Continuous Media* (Pergamon, Oxford, 1978).

[107] G. E. Pikus and A. N. Titkov, in *Optical Orientation*, edited by F. Meier and B. P. Zakharchenia (Elsevier, Amsterdam, 1984), Chap. 3.